

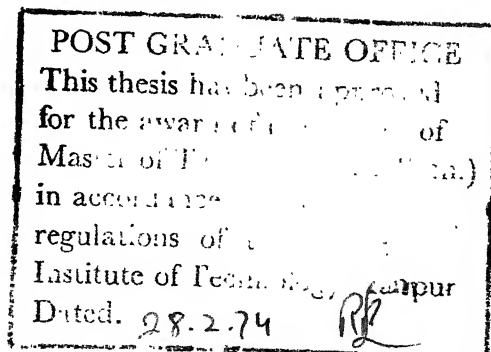
DECOMPOSITION PRESSURES AND TERMINAL SOLID SOLUBILITY OF HYDROGEN IN Zr-10 Wt % Nb ALLOY

A Thesis Submitted
In Partial Fulfilment of the Requirements
for the Degree of
MASTER OF TECHNOLOGY

CENTRAL LIBRARY
INDIAN INSTITUTE OF TECHNOLOGY KANPUR

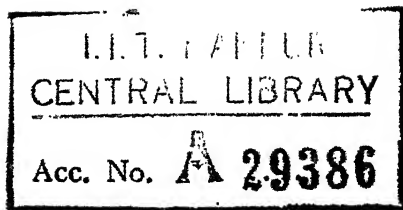
By
SATISH PRAKASH SINGHAL

33823



to the

DEPARTMENT METALLURGICAL ENGINEERING
INDIAN INSTITUTE OF TECHNOLOGY KANPUR



Thesis
669.96735
Si64

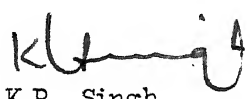
25 APR 1974

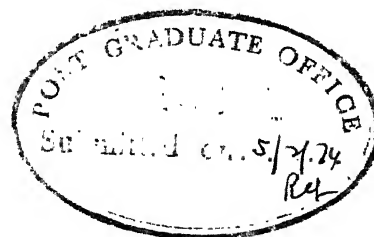
ME-1974-M-SIN-DEC


CERTIFICATE

This is to certify that this work entitled,
 "Decomposition Pressures and terminal solid solubility of
 hydrogen in Zr-10 wt % Nb alloy" has been carried out by
 Satish Prakash Singhal, under my supervision and has not
 been submitted elsewhere for a degree.

Kanpur
 February, 1974


 Dr. K.P. Singh
 Professor & Head
 Department of Metallurgical Engineering
 Indian Institute of Technology, Kanpur



<p>POST GRADUATE OFFICE</p> <p>This thesis has been submitted for the degree of Master of Science in accordance with the regulations of the Institute of Technology, Kanpur Dated. 28-2-74</p> <p></p>

ACKNOWLEDGEMENTS

I express my sincere thanks to Professor K.P. Singh for encouragement and guidance provided by him during the course of this work.

I am deeply indebted to my friends Mr. S.K. Si and Dr. V.K. Sinha for their indispensable help and suggestions from time to time. Some interesting discussions with Dr. A.K. Jena are very gratefully acknowledged.

I am also very much thankful to Dr. K. Shri Ram and staff of Central Nuclear Laboratories for availing me liquid nitrogen for the present work at various times. In the end I am grateful to Mr. Subramaniam for glass blowing and Mr. S.N. Gupta for his care and keen interest in typing the manuscript.

AUTHOR

C O N T E N T S

CHAPTER I	INTRODUCTION	1
CHAPTER II	LITERATURE REVIEW	
	2.1 Introduction	5
	2.2 Terminal Solid Solubility of Hydrogen in Zr and Zr-Nb alloys	6
CHAPTER III	EXPERIMENTALS	
	3.1 Experimental Set-up	9
	3.2 Materials	18
	3.3 Experimental Procedure	18
CHAPTER IV	RESULTS AND DISCUSSIONS	
	4.1 Introduction	24
	4.2 Terminal Solid Solubility of Hydrogen in Zr-10Wt% Nb Alloy	33
CHAPTER V	CONCLUSIONS	44
REFERENCES		45
APPENDIX		49

LIST OF TABLES

<u>Table</u>	<u>Page</u>
1. Compositions of the, (Zr-10Wt% Nb)-H ₂ Alloys Used for Decomposition Pressure Studies	25
2. Decomposition Pressure-Composition-Temperature data for the (Zr-10Wt% Nb)- H 0.0251 Alloy	26
3. Decomposition Pressure-Composition-Temperature data for the (Zr-10Wt% Nb) - H 0.0356 Alloy	27
4. Decomposition Pressure - Composition - Temperature data for the (Zr-10Wt% Nb) - H 0.0433 Alloy	28
5. Decomposition Pressure-Composition-Temperature data for the (Zr-10Wt% Nb) - H 0.0527 Alloy	29
6. Decomposition Pressure-Composition-Temperature data for the (Zr-10Wt% Nb) - 4 0.0613 Alloy	30
7. Terminal Solid Solubility (TSS) of Hydrogen in the Zr-10Wt% Nb Alloy	38

LIST OF FIGURES

<u>Figure</u>		<u>Page</u>
1(a)	Apparatus for determining decomposition pressures of hydrides	13
1(b)	Schematic plot of mercury manometer and enlarged view of diffusion pumps, K & L of Fig. 1(a)	14
1(c)	Two stage McLeod gauge	15
1(d)	Photograph of the apparatus for determining decomposition pressures of hydrides	16
2.	Isothermal pressures against at% hydrogen for Zr-10Wt% Nb alloy in temperature range 425 to 575°C.	31
3.	Isothermal pressure against at% hydrogen for Zr-10Wt% Nb alloy at 600°C	32
4.	Plot of decomposition pressure Vs. reciprocal of temperature for (Zr-10Wt% Nb)-H 0.0433 alloy	34
5.	Plot of decomposition pressure Vs. reciprocal of temperature for (Zr-10Wt% Nb)-H 0.0613 alloy	35
6.	Plot of decomposition pressure Vs. reciprocal of temperature for (Zr-10Wt% Nb)-H 0.0527 alloy	36
7.	Plot of decomposition pressure Vs. reciprocal of temperature for (Zr-10Wt% Nb) H 0.0433 and (Zr-10Wt% Nb) - H 0.0251 alloys	37
8.	TSS boundaries $(\alpha + \beta \text{ Nb}) - (\alpha + \beta_{\text{Nb}} + \delta)$ for the (Zr-2.5Wt% Nb)-H ₂ systems and $\alpha - (\alpha + \delta)$ for Zr-H ₂ system	39

9.

FigurePage

- | | | |
|-----|--|----|
| 9. | Plot of $\ln C_T$ against $1/T^\circ K$ for $(\chi + \delta Nb) - (\chi + \delta Nb + \delta)$
TSS boundary in the $(Zr-2.5Wt\% Nb)-H_2$ and
$(Zr-10Wt\% Nb) - H_2$ systems; and for $\delta - (\chi + \delta)$ TSS
boundary in $Zr-H_2$ system | 40 |
| 10. | The equilibrium phase relations in zirconium-
hydrogen system | 50 |
| 11. | The equilibrium phase diagram of Zr-Nb system | 51 |
| 12. | The equilibrium phase relations in niobium -
hydrogen system | 52 |

ABSTRACT

Decomposition pressure studies were made on five (Zr-10wt% Nb) - H_2 alloys (with 2.45, 3.44, 4.15, 5.0 and 5.78 at% H), in the temperature range from 425° to 675°C. The terminal solid solubility (TSS) of hydrogen in the alloy was determined with the help of Vant Hoff plot between logarithm of decomposition pressure and reciprocal of temperature. Presence of 10wt% Nb does not seem to have affected the TSS of hydrogen in the alloy, as compared to unalloyed zirconium.

The mean enthalpy of formation of δ hydride from saturated Zr-10wt% Nb alloy, $\Delta\bar{H}_{\alpha \rightarrow \delta}$, was computed to be, -40.38 ± 1 K.Cal/mole H_2 .

CHAPTER I

INTRODUCTION

Zirconium and its alloys are used primarily for manufacture of pressure tubings and cladding sheaths for nuclear fuel rods. The constructional materials are required in nuclear reactors to protect the fuel rods from corrosion, to provide heat transfer surface and to provide a structural support. Such materials must have suitable mechanical properties and resistance to corrosion by heat transfer medium at the operating temperature. In addition, these materials must not absorb neutrons excessively, as, otherwise the chain reaction to keep fission process continued will be stopped. This last requirement is very critical and is met only by four metals, namely, aluminium, zirconium, magnesium and beryllium. Aluminium and magnesium can be used but at elevated temperatures both lose strength as well as corrosion resistance. Beryllium ores are very scarce and the metal is very costly (1). Moreover, mechanical properties of beryllium are inferior to those of zirconium, and the fabrication techniques for the former are not very developed. The metal zirconium possesses satisfactory nuclear and physical characteristics and good mechanical properties at room temperature as well as at high temperatures. The structural stability of zirconium at high temperatures, as compared to other three metals (Al, Be and Mg), provides a possibility of running the reactors at higher temperatures. This will improve the thermal efficiency of turbines attached with the reactor. The property of corrosion

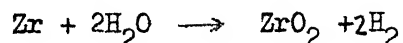
resistance by heat transfer medium in a wide temperature range and development of satisfactory fabrication techniques have further increased the potential of zirconium as a structural material for nuclear reactors.

However, one of the biggest problems encountered with unalloyed zirconium is the drastic increase in its oxidation rate even due to the slight contamination with very common impurities like nitrogen and carbon⁽⁴⁾. Therefore, it was felt that for improved corrosion resistance the metal must be toned up by alloying additions. The development of zirconium base alloys like Zircaloy-1, Zircaloy-2, Zircaloy-3, nickel free Zircaloy-2 and Zircaloy-4 was a major break-through in this context⁽³⁾. In all the above alloys tin is the major alloying addition with iron, nickel and chromium as minor ternary additions. Out of these alloys, Zircaloy-2 has been universally accepted as a potential material for fuel claddings and pressure tubings because of its good corrosion resistance and better mechanical strength. Nevertheless there had been ample amount of work for further development of zirconium base alloys (4,7,8,9,10,11) of higher strength and corrosion resistance so that the wall thickness of pressure tubing and fuel cladding can be reduced and maximum burn up can be achieved inside the reactor.

The possibility of use of Nb as an alloying element to improve mechanical strength and corrosion resistance of zirconium was first investigated by the Russian workers^(5,6). The studies made by various authors^(5,6,7,8,9,10) suggest that out of available

zirconium base alloys perhaps Zr-2.5 wt% Nb is the most promising and potential competitor to Zircalloy-2. The Zr-2.5 wt% Nb alloy possesses about 40% higher tensile strength in heat treated condition^(4,7,8,9,10) along with good ductility and creep resistance. The addition of 2.5 wt% Nb while not affecting the neutron capture cross section area more than marginally, makes it possible to use thinner fuel cans and pressure tubings due to the improved mechanical properties and corrosion resistance of the alloy⁽³⁾. Such reduction in wall thickness not only improves neutron economy but also maximizes the burn up of reactor because of reduction in volume of nonfissile material within the reactor core.

When zirconium base alloys are used in high temperature water or steam environment they readily absorb hydrogen by virtue of the reaction



The absorption of this hydrogen leads to precipitation of zirconium hydride which causes embrittlement of zirconium, and its alloys when cooled to ambient temperatures^(11,12,13,14). Such embrittlement may lead to disastrous consequences owing to the brittle failure of zirconium base alloy tubes. This has been one of the main problems in the use of zirconium base alloys for reactor purposes.

The interest in hydrogen solubility of zirconium base alloys stems basically from the fact that possibility and amount of

hydride precipitation in an alloy is dependent upon the terminal solid solubility of hydrogen in that alloy. Since embrittling effect due to presence of hydride depends upon its amount, the effect of alloying additions on TSS of hydrogen in zirconium is very crucial. Therefore, the study of the effect of most promising alloying element niobium on TSS of hydrogen in zirconium is of great interest.

There had been considerable work on TSS of hydrogen in Zircalloys and Zr-2.5 wt% Nb alloy^(16,17,18,19,20,32). However, the results obtained by various workers as to the effect of niobium on the terminal solid solubility of hydrogen in Zr, are in considerable disagreement. Attempts have not been made to study the effect of higher Nb (more than 2.5 wt%) content, on TSS of hydrogen in zirconium, which perhaps could have given an indication about qualitative effect of Nb on hydrogen solubility in zirconium. The present work, therefore, was carried out to study TSS of hydrogen in a Zr-10 wt% Nb alloys.

CHAPTER II

LITERATURE REVIEW

2.1 INTRODUCTION:

The work on Zr-H₂ system was started as early as in 1929. The first pioneering work in this field was done by Hagg³⁵, who by using X-ray diffraction technique, identified three hydride phases in this system. Later work in this field is by Hall et al³⁶, Edwards et al³⁷ and by Edwards and Le Vesque³⁸. These workers, however, could not recognise some of the most inherent features of Zr-H₂ system, because zirconium available these days was highly contaminated with oxygen and hafnium. Later on, work of Gulbransen & Andrew^{21,39} Ells and Mc Quillan²², Vaughan and Bridge⁴⁰, Libowitz⁴¹, Beck⁴² Lagranges et al²⁹, Moore & Young⁴⁹ and Mishra et al⁴³, established almost the complete phase diagram of Zr-H₂ system. An excellent review of work on Zr-H₂ system has been provided by Beck and Mueller². Since zirconium base alloys forms a potential class of material for nuclear reactor applications, the study of the effect of alloying elements on phase equilibria in Zr-H₂ system is of great interest. Studies of effect of oxygen on Zr-H₂ system were initiated by Hall et al³⁶ and Edwards et al³⁸. More systematic investigations as to the effect of oxygen were carried out by Brown and Hardie⁴⁴ and Singh and Parr⁴⁵. Beck and Mueller² have reviewed the effect of various alloying elements on phase boundaries in Zr-H₂ system. The effect of Nb on β -(β + δ) and (β + δ) - δ boundaries has been investigated by Sinha and Singh^{46,47} in great details.

2.2 TERMINAL SOLID SOLUBILITY OF HYDROGEN IN Zr AND Zr-Nb ALLOYS:

The terminal solid solubility (TSS) boundaries $\alpha-(\alpha+\delta)$ and $\alpha-(\alpha+\beta)$ in unalloyed Zr-H₂ system have been more or less established through the works of Gulbransen and Andrew²¹ and Ells and Mc Quillan²². They used decomposition pressure measurement technique to establish TSS boundaries. Measurements have been made on $\alpha-(\alpha+\delta)$ boundary using other techniques^{17,18,23,24} and results are in close agreement to those of Gulbransen and Andrew²¹. However diffusion penetration experiments^{26,2} and dilatometric cooling curves^{16,17,23} have given somewhat higher results. The dilatometric heating curves in general are in agreement with work of Gulbransen and Andrew²¹; but the cooling curves show a shift of the boundary to a lower temperature by 20 to 70°C. Erickson¹⁸ has indicated that probably TSS determined by dilatometric heating curves gives the equilibrium boundary; while cooling curves gives the boundary for precipitation of a metastable hydride from super saturated solid solution. Terminal solid solubility of hydrogen in unalloyed zirconium, above the eutectoid temperature, was studied by La Granges et al²⁹ and Erickson and Hardie¹⁷. The results of these workers are in close agreement to that of Ells and Mc Quillan²².

Several investigators^{16,17,18,19,20,30,32} have attempted to establish TSS of hydrogen in Zr-2.5 wt% Nb alloy below eutectoid temperature. Brown¹⁶ using dilatometric cooling curves established that solubility of hydrogen is greatly exceeded in

Zr-2.5 wt% Nb alloy as compared to unalloyed zirconium. Erickson¹⁸ has attributed this increase in solubility to super saturation. Sawatzky³⁰ established TSS boundary of hydrogen in Zr-2.5 wt% Nb alloy using layer technique and reported that though presence of niobium increased the hydrogen solubility; but increase is not as much as reported by Brown¹⁶. The results of Erickson and Hardie¹⁷ based on dilatometric cooling curves were in fair agreement to that of Sawatzky³⁰; however their heating curves showed that Zr and Zr-2.5 wt% Nb had identical TSS limits.

Sawatzky and Wilkins¹⁹ redetermined this boundary, using a thermal gradient method and found that TSS of hydrogen in Zr and Zr-2.5 wt% Nb were essentially same. Erickson's¹⁸ equilibrium pressure isotherm results showed a higher TSS limit in the Zr-2.5 wt% Nb-H₂ system, than in the Zr-H₂ system. Coates and Erickson⁴⁸ carried out measurements on TSS of hydrogen in Zr-2.5 wt% Nb alloy by isothermal technique during heating and cooling cycles. It was found that TSS measured during cooling cycle is same as isothermal TSS reported¹⁸, while TSS measured on heating cycle agrees with the accepted solubility limit in zirconium. Kearns²⁸ has reviewed the available hydrogen solubility data on zirconium, zircalloy-2 and zircalloy-4, below eutectoid temperature and he showed that terminal solid solubilities were nearly same for all the three materials. Erickson¹⁸ has concluded that probably equilibrium TSS of hydrogen in zirconium is not greatly affected either by the presence of niobium and/or by changes in oxygen

content. Work of Erickson and Hardie¹⁷ also suggests that low level alloying of zirconium does not significantly affect the TSS boundary in Zr-H₂ system.

Sinha³² determined TSS boundary of hydrogen in Zr-2.5 wt% Nb alloy, using decomposition pressure technique, below and above eutectoid temperature. It has been reported that presence of niobium increases TSS of hydrogen in the alloy; especially in the temperature range of 425°C to 700°C. Extrapolation of TSS boundaries above and below eutectoid temperature suggests that the hydrogen solubility in Zr-2.5 wt% Nb is maximum at the eutectoid temperature of Zr-H₂ system. This value is proposed to be about 8.5 at %H.³² The established TSS of hydrogen in unalloyed Zr-H₂ at the eutectoid² temperature is only 6.1 at%. The results on TSS of hydrogen in Zr-2.5 wt% Nb obtained by Sinha³² are in qualitative agreement with those of Brown¹⁶ and Erickson¹⁸. However the reported³² increase in TSS boundary is not as much as found by Brown¹⁶ and Erickson¹⁸.

The discrepancies in the results on TSS of hydrogen as reported by various workers, may be ascribed to differing experimental techniques and differences in compositions of the starting materials. The present review suggests that the effect of Nb on TSS of hydrogen in zirconium is still a matter of great conjecture. There are disagreements among various workers as to the effect of Nb, qualitatively as well as quantitatively. With this end in view it was considered worthwhile to study the effect of niobium on TSS of hydrogen in zirconium, with higher niobium contents. Thus the present investigation to establish the TSS of hydrogen in a Zr-10 wt% Nb alloy below eutectoid temperature, was carried out by means of decomposition pressure technique.

CHAPTER III

EXPERIMENTALS

3.1 EXPERIMENTAL SET UP:

Zirconium and its alloys are highly reactive and can easily get contaminated with atmospheric gases like nitrogen and oxygen. Such contaminations may affect the hydrogen solubility of zirconium and its alloys. Moreover, TSS measurement by decomposition pressure technique needs measurement of very low partial pressures of hydrogen. This requires a gas handling apparatus essentially consisting of the following parts:

- (i) high vacuum pumping accessories,
- (ii) pure hydrogen source,
- (iii) pressure measuring devices,
- (iv) high vacuum manifold,
- (v) means of heating the specimen and control of temperature.

An apparatus incorporating all the above parts and fulfilling necessary conditions of experiment, was designed and fabricated by Sinha⁽³²⁾. The same apparatus was used in the present investigation (Fig. No.1a to 1d). The various components of the system are being described here:

(i) High Vacuum Pumping Accessories:

The main function of high vacuum pumping accessories is to create an initial vacuum in the system so that unwanted gases like oxygen and nitrogen are reduced to a minimum concentration. This part of the apparatus consisted of two double stage mercury diffusion pumps (K & L), and a two stage Welch Duo Seal, Model 1405

10

backing mechanical pump. Liquid nitrogen traps were used at suitable junctions along with the mercury diffusion pumps. The mechanical pump used has a capacity of 33.4 liters per minute and an ultimate pressure of 0.5 micron.

(ii) The Pure Hydrogen Source:

Pure hydrogen was obtained by heating and dissociating titanium hydride in a vacuum better than 10^{-6} mm Hg. To prepare titanium hydride, cylinder hydrogen was passed over copper turnings heated to 450°C to remove any oxygen. The oxygen free hydrogen thus obtained, was reacted, with titanium granules at 850°C to form titanium hydride. Titanium granules were cooled down to room temperature in the presence of excess hydrogen so that complete saturation with hydrogen took place.

(iii) Pressure Measuring Devices:

The system contained three pressure measuring devices namely a U-tube manometer, a McLeod gauge and an ionization gauge. In the U-tube manometer, the triple distilled mercury was used as manometric fluid and it could measure pressure in the range of 3 mm Hg to 760 mm Hg. To measure system pressures below 3 mm Hg a two stage McLeod gauge with triple distilled mercury as gauge fluid was used. The dimensions of the McLeod gauge (Fig.No. 1-C) were suitable for the pressure range of interest in the present investigation. From the known volumes V_1 , V_2 and V_3 in c.c at the first and second cut off (Fig. No. 1-C) the system pressure⁽³²⁾ at any instant due to the middle capillary reading was obtained from

the relation,

$$P = \frac{\pi r^2 h_1^2 (V_2 + V_3)}{4 V_1 V_3} \text{ cm Hg} \quad \dots \quad (3.1)$$

and that due to the extreme right capillary from the relation,

$$P = \frac{\pi r^2 h_2^2 (V_2 + V_3)}{4 V_1 V_2} \text{ cm Hg} \quad \dots \quad (3.2)$$

where

r is the radius of the capillary bore in cm,

h_1 is the height difference in cms between the sealed end AA and the mercury level in the middle capillary,

h_2 is the height difference between the sealed end AA and mercury level in the extreme right capillary.

Though the pressure reading sensitivity of the additional extreme right capillary is only V_2/V_3 of that of the middle capillary, the operating range is obviously greater by a factor of V_3/V_2 .

The design and calibration of the McLeod gauge used has been described elsewhere⁽³²⁾. The various volumes V_1 , V_2 and V_3 were found to be equal to 305.0, 0.22 and 6.205 cm³ respectively. It was found that this McLeod gauge could be used to measure the pressures in a range from 3 mm Hg to 10^{-6} mm Hg. This range was quite adequate for present work. The McLeod gauge pressure readings were found to be accurate and reproducible to ± 0.5 , ± 0.6 , ± 2.0 and ± 6.0 % at pressures of 10^{-2} , 10^{-3} , 10^{-4} and 10^{-5} mm Hg respectively.

A Veeco ionization gauge, type RG-21X, was attached to the system and was used only for measuring the order of vacuum during initial evacuation of the apparatus. The decomposition pressure

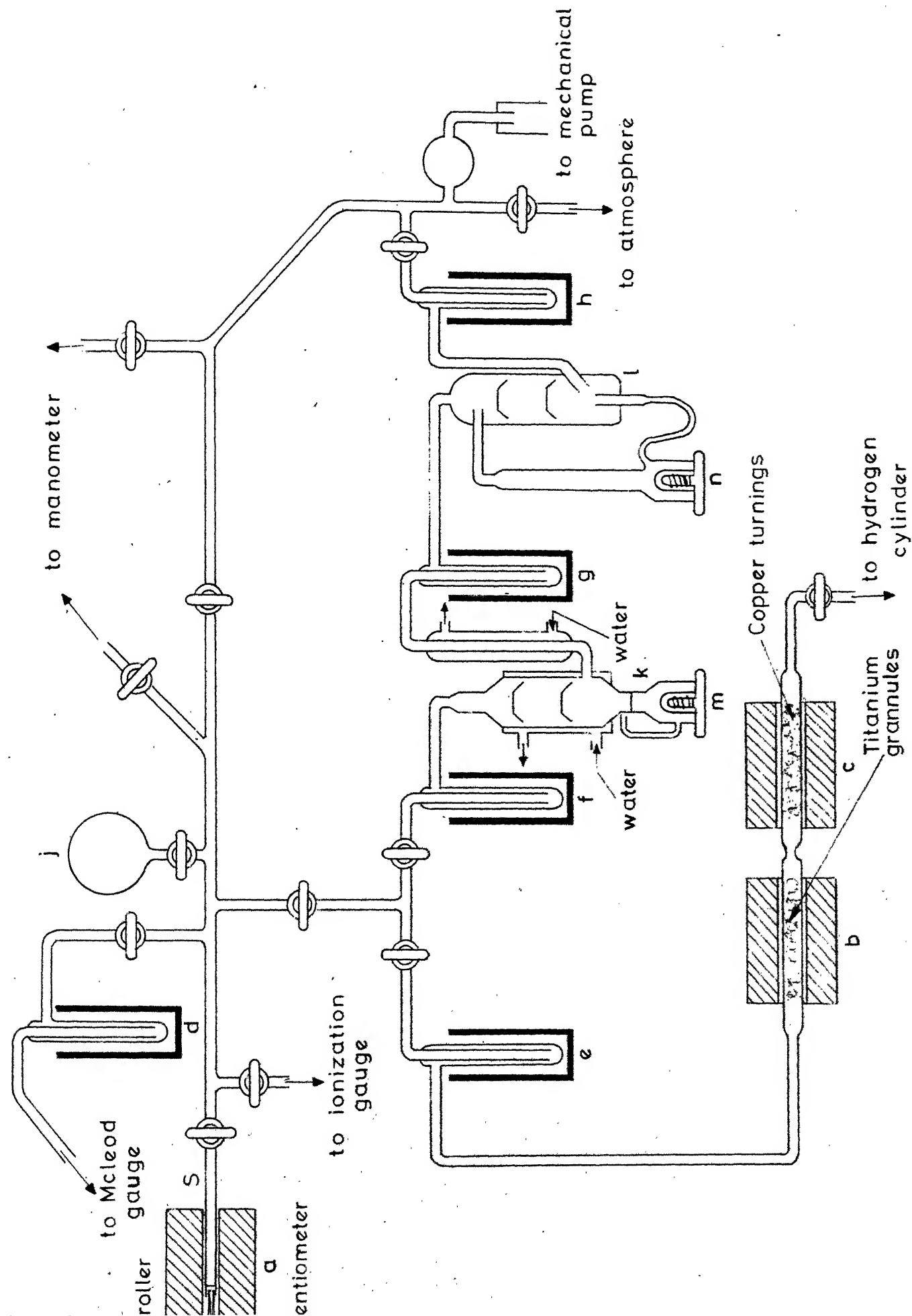


Fig.1(a) Apparatus for determining decomposition pressure of hydrides.

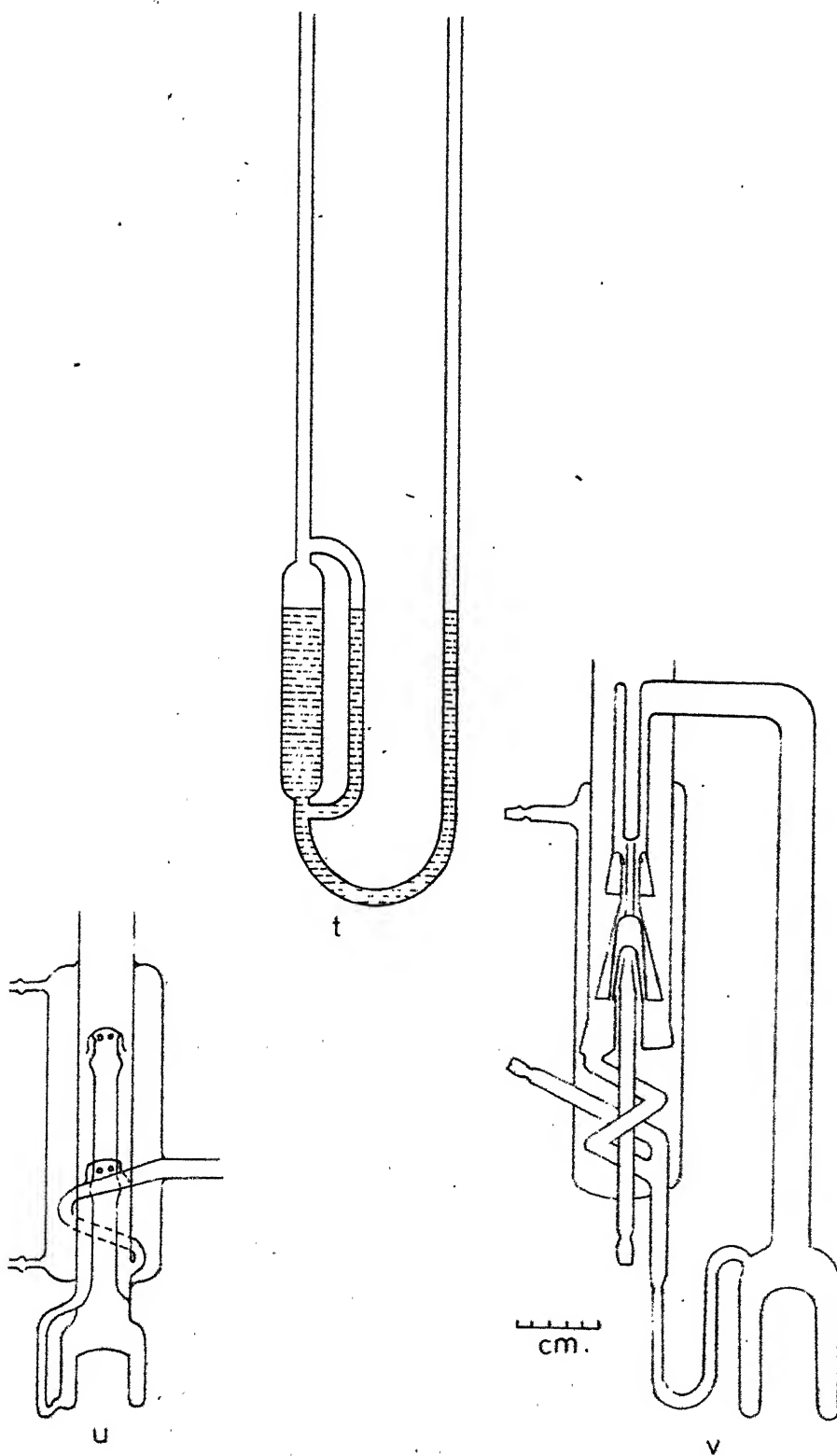
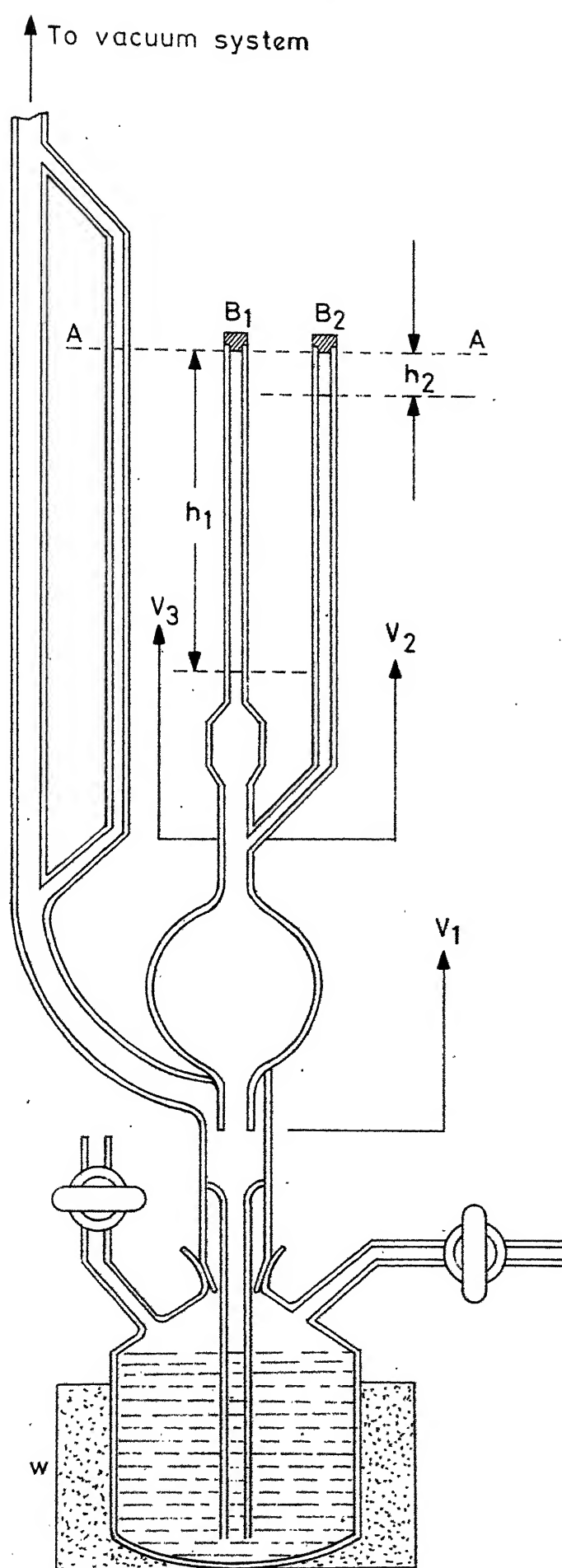


Fig.1(b) Schematic plot of mercury manometer and enlarged view of diffusion pumps.



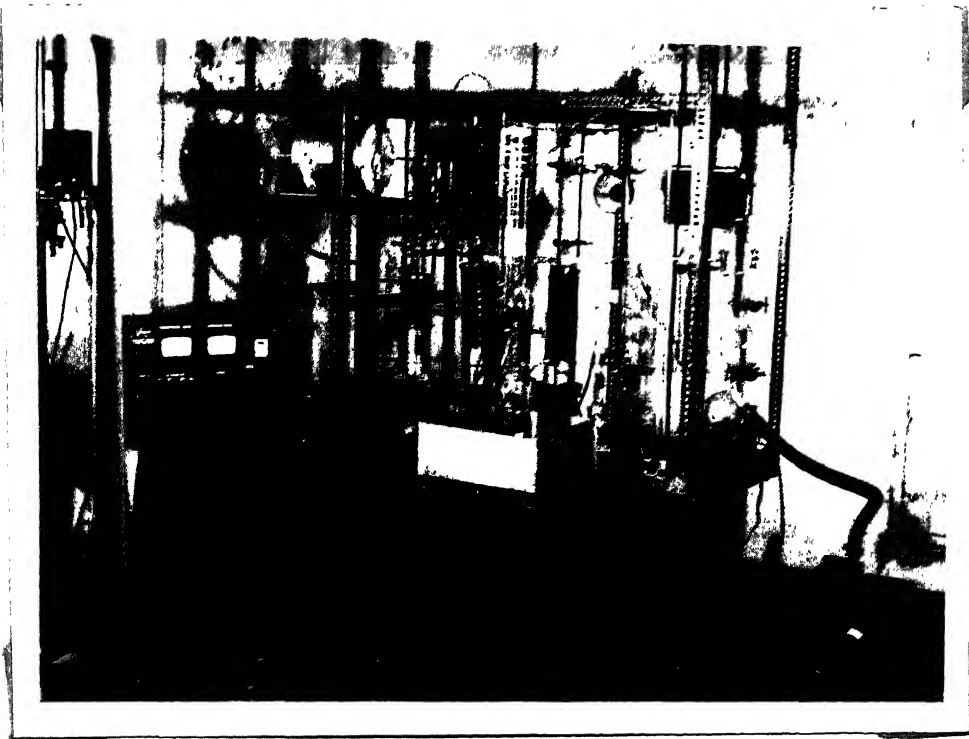


Fig. 1(d): Photograph of the apparatus for determining decomposition pressures of hydrides.

measurements were done only with the McLeod gauge.

(iv) High Vacuum Manifold:

The high vacuum manifold formed the most important part of the present gas handling apparatus. The vacuum pumping accessories, the pure hydrogen source, and the pressure measuring devices could be connected or isolated from high vacuum manifold by a set of stop cocks. The stop cocks connected to the manifold and the other parts of the system were all certified Corning high vacuum stop cocks. Previously degassed T type Apiezon grease was used to lubricate the stop cocks. A pyrex bulb j, with a calibrated volume of $1044.4 \pm 1 \text{ c.c.}$ was fused to the high vacuum manifold. This bulb served two purposes; first to calibrate the volumes of the various parts of the system, and second to store the pure hydrogen required for hydriding the specimens. The high vacuum manifold was connected to the quartz specimen tube, s, through a graded seal.

(v) Means of Heating the Specimen and Control and Measurement of Temperature:

The specimen tube, s, was placed in a resistance heated movable, horizontal axis tube furnace. The end portion of the specimen tube could be kept in a constant temperature zone within the furnace. It was observed that in a constant temperature zone of three centimeters, a maximum difference of about 1°C existed at 950°C . The temperature of this specimen zone was controlled better than $\pm 1^\circ\text{C}$ by putting a suitable resistance across the relay of an Electromax controller (Model No. 6251) activated by a chromel

alumel thermocouple. Another chromel alumel thermocouple was used to measure the temperature of the constant temperature heating zone where the specimen was placed in the specimen tube. The calibration of the control, as well as the measuring thermocouple was checked with a standard thermocouple, before use. The e.m.f. of the measuring thermocouple was measured by a potentiometer with a sensitivity of ± 0.001 mV.

3.2 Materials:

The Zr-10 Wt% Nb alloy prepared from reactor grade Zr and Nb was received from Bhabha Atomic Research Centre, Bombay. The alloy was arc melted three or four times to ensure homogeneity. A carefully purified argon gas atmosphere was maintained during melting. The alloy was obtained in the form of buttons weighing 100 to 150 gms.

3.3 Experimental Procedure:

A complete experimental run involved four main steps:

- (i) specimen preparation,
- (ii) evacuation of the system,
- (iii) hydriding the specimen, and
- (iv) decomposition pressure measurements.

All these steps are discussed in the following sections:

(i) Specimen Preparation:

Thin strips of the alloy were cut from the alloy button by means of a hacksaw. Both the surfaces of the thin specimens were ground on emery papers (up to 4/0 grade) to polish the surfaces.

The specimens were washed with high purity acetone, dried and finally weighed in a Mettler microoptical balance, model M5. The balance had a readability of 0.001 mg. with an accuracy of 0.001 mg. Specimens used for the experiments were about 1 cm long and 0.4 cm wide and weighed approximately 200 to 350 mg. The specimens were transferred to specimen tube, immediately after preparation and weighing, without touching with hands, to keep the surface perfectly bright. The specimen tube was fused to high vacuum manifold every time the specimen was changed. Extreme care was taken in fusing the specimen tube to manifold so that volume of the manifold do not change during the process of glass blowing.

(ii) Evacuation of the System:

Because of their highly reactive nature zirconium and its alloys can easily be contaminated with common atmospheric gases like oxygen and nitrogen. Therefore, in a work of this kind, it is necessary to ensure that the apparatus is as free from contaminating gases as possible. It was not possible to bake out the complete apparatus; but as much of it as possible was heated under vacuum and the whole system was continuously evacuated at a vacuum of 10^{-6} mm Hg for several hours. The use of two mercury diffusion pumps, L and K in series, made evacuation process very efficient. It was observed that the system would reach a vacuum of the order of 10^{-7} mm Hg within an hour, and when isolated from pumping accessories it would hold a vacuum of 10^{-6} mm Hg to 10^{-5} mmHg for several days. During entire experimentation the room temperature

was never allowed to go beyond 25°C ; so that grease used in stop cocks might not soften and lead to the leakage. A Veeco RG 21X ionization gauge was used to measure the initial evacuation of the system.

(iii) Hydriding the Specimens:

The volumes of the entire apparatus, and its various parts were determined by a gas expansion method in terms of the known volume of the bulb, j, using mercury nanometer, with appropriate corrections. After the initial evacuation as per above description the system was flushed four to five times with pure hydrogen and was evacuated every time to a vacuum of the order of 10^{-7} mm Hg. The specimen was then annealed at 900°C in a running vacuum of 10^{-6} mm Hg for about $\frac{1}{2}$ an hour. The annealing treatment not only relieves strains induced during polishing but also completely homogenises the specimen. After annealing the specimen was cooled down to the room temperature.

To prepare a Zr-10Wt% Nb- H_2 alloy of predetermined hydrogen concentration a known and previously calculated amount of hydrogen was introduced into the system. The pure hydrogen produced by decomposition of titanium hydride was passed through a liquid nitrogen trap to remove any moisture which might have been absorbed by quartz tube containing titanium granules. The specimen tube was then inserted into the furnace at 900°C and the alloy was allowed to react with the known amount of hydrogen. Specimens were found to absorb almost all the hydrogen within seconds. Furnace temperature was then lowered to nearly 500°C and held there for

about 24 hrs for complete homogenization. The specimen was next cooled down to room temperature. The pressure of unabsorbed hydrogen was measured with the help of McLeod gauge; and its quantity was computed with the help of gas law. Since the initial number of moles of hydrogen and the number of moles of unabsorbed hydrogen were known, the quantity of hydrogen absorbed by the specimen could be obtained. From these values the composition of a particular Zr-10wt% Nb-H₂ alloy was determined. The composition of the hydrided specimen with all care, could be computed within a maximum uncertainty of 0.15 to 0.2 wt % hydrogen. Five alloys of different hydrogen concentration were prepared and studied for their decomposition pressure as a function of temperature. These Zr-10wt% Nb-H₂ alloys are listed in table 1. After each experimental run, the hydrided Zr-10wt% Nb-H₂ alloy was weighed on the microoptical balance. In each case hydrogen content of the specimen determined by the gain in weight tallied within about 1% to that computed earlier by gas law.

(iv) Decomposition Pressure Measurements:

Decomposition pressure studies were started directly after hydriding the specimens to avoid the contamination. To measure the decomposition pressures, the Zr-10wt% Nb-H₂ specimen was heated in the closed system and changes of pressure occurring with specimen temperature was noted. Usually measurements were done at an interval of 25°C; but near the suspected transition points it was reduced to 10 to 15°C. Decomposition reaction in Zr-10wt% Nb-H₂

alloys was slow as compared to Zr-2.5wt% Nb-H₂ or Zr-H₂ alloys. Decomposition reaction above 500°C was fast; but in initial stages decomposition pressure fluctuated quite a bit. After 8-10 hrs. it was found to assume the equilibrium value. Below 500°C the decomposition was quite slow and at each temperature complete assessment and confirmation of decomposition pressure took 2 to 3 days. Readings were finally noted down only after observing that same reading holds for 8-10 hours at particular temperature. Each decomposition pressure run took around 15-20 days. Cooling runs were also made to check the reproducibility of data and a fair agreement was found between heating and cooling cycle data.

Since decomposition pressure technique involves heating of a particular metal-hydrogen alloy in a closed system, the hydrogen content of specimen changes as temperature is raised. The specimen weight was optimized in such a way that no significant change in specimen composition could occur up to a decomposition pressure of about 10^{-3} mm Hg. At higher decomposition pressures the composition changes were minimized by isolating the ionization gauge and bulb j from the system and thus reducing its volume from 1842 to 447 cc. It was possible to compute the hydrogen concentration of alloy at any pressure with the help of gas law making appropriate corrections.

Although in principle the complete investigation could be done using a single specimen of Zr-10wt% Nb alloy, in practice no

specimen was used more than once to avoid the error in estimating the hydrogen content and degree of contamination with oxygen and nitrogen; both of which may increase with each run.

CHAPTER IV

RESULTS AND DISCUSSIONS

4.1 INTRODUCTION

The results of present investigation have been presented in the form of Van't Hoff plots for various (Zr-10Wt%Nb)-H₂ alloys. The equilibrium decomposition pressure (P), for a metal-hydrogen alloy can be represented as a function of temperature with the help of equation (21)

$$\frac{1}{2} \left[\frac{\partial \ln P}{\partial (1/T)} \right]_{X_H} = \frac{\Delta H}{R} \quad \dots \quad 4.1$$

where X_H = atomic fraction of hydrogen in the alloy.

For Zr-H₂ system, ΔH in above equation is the relative partial molal enthalpy of hydrogen ($\bar{H}_{H(\alpha)}^\circ - \frac{1}{2} H_{H_2(gas)}^\circ$), if alloy is in single phase (α) region, and ($\bar{H}_{H(\gamma)}^\circ - \frac{1}{2} H_{H_2(gas)}^\circ$), if alloy is in two phase ($\alpha + \gamma$) region. Hence a plot of $\ln P$ Vs $1/T$ will undergo a change of slope whenever a particular Zr-H₂ alloy passes from one phase field to another, and the temperature at which the change of slope occurs, defines the location of phase boundary. The above form of equation (4.1) can be used to determine TSS of hydrogen in (Zr-10Wt% Nb)-H₂ system also. The complete TSS boundary can be determined by measuring the decomposition pressures of a series of (Zr-10Wt% Nb)-H₂ alloys as a function of temperature.

In present investigation five (Zr-10Wt% Nb)-H₂ alloys (Table-1), were taken for decomposition pressure studies and P-C-T data for these alloys are listed in Tables 2 to 6. Since composition of the specimens changes with increasing temperature

Table 1

Compositions of the (Zr-10wt%Nb) - H₂
Alloys Used for Decomposition Pressure Studies

Alloy Number	Composition of the Zr-10Wt% Nb-H ₂ alloys			ppm H ₂ by weight
	Wt % H	at % H	$\frac{\text{H}}{\text{Zr-10Wt\% Nb}}$ atomic ratio	
1	.0277	2.45	0.0251	277
2	0.0393	3.44	0.0356	393
3	0.0477	4.15	0.0433	477
4	0.0580	5.00	0.0527	580
5	0.0676	5.78	0.0613	676

Table 2

Decomposition pressure-Composition-Temperature data for the

(Zr-10Wt%Nb) - H 0.0251 alloy

Temperature °C	Decomposition pressure in mm Hg	Composition at %H	Interpolated decomposition press- ure, p, in mm Hg for constant composition of the alloy (2.45 at %H)
425.0	3.76×10^{-4}	2.445	3.76×10^{-4}
450.0	8.08×10^{-4}	2.443	8.08×10^{-4}
475.0	1.95×10^{-3}	2.438	1.98×10^{-3}
500.0	4.034×10^{-3}	2.428	4.08×10^{-3}
500.0*	4.00×10^{-3}	2.428	
525.0	6.62×10^{-3}	2.424	6.75×10^{-3}
550.0	1.12×10^{-2}	2.419	1.18×10^{-2}
550.0*	1.10×10^{-2}	2.419	
575.0	1.74×10^{-2}	2.411	1.80×10^{-2}
600	2.33×10^{-2}	2.403	2.38×10^{-2}

* Data taken during cooling run

Table 3

Decomposition Pressure-Composition-Temperature data for the

(Zr-10Wt% Nb) - H 0.0356 alloy

Temperature °C	Decomposition pressure in mm. Hg	Composition at % H	Interpolated decomposition pressure for cons- tant composition of the alloy (3.44 at%H)
425.0	6.43×10^{-4}	3.432	6.43×10^{-4}
450.0	2.06×10^{-3}	3.421	2.06×10^{-3}
475.0	4.70×10^{-3}	3.396	4.77×10^{-3}
490.0	6.90×10^{-3}	3.383	7.0×10^{-3}
500.0	8.32×10^{-3}	3.371	9.0×10^{-3}
525.0	1.46×10^{-2}	3.357	1.55×10^{-2}
550.0	2.45×10^{-2}	3.336	2.60×10^{-2}
575.0	3.74×10^{-2}	3.309	4.0×10^{-2}

Decomposition Pressure-Composition-Temperature data for the
(Zr-10Wt% Nb) - Ho.0433 alloy

Temperature °C	Decomposition pressure in mm. Hg	Composition at % H	Interpolated decomposition pressure for cons- tant composition of the alloy (4.15 at % H).
425.0	6.79×10^{-4}	4.148	6.79×10^{-4}
450.0	1.65×10^{-3}	4.143	1.65×10^{-3}
475.0	5.64×10^{-3}	4.126	5.64×10^{-3}
490.0	8.50×10^{-3}	4.113	8.50×10^{-3}
500.0	1.33×10^{-2}	4.091	1.33×10^{-2}
525.0	1.91×10^{-2}	4.083	2.10×10^{-2}
550.0	3.22×10^{-2}	4.068	3.60×10^{-2}
575.0	5.14×10^{-2}	4.045	5.30×10^{-2}

Table 5

Decomposition Pressure-Composition-Temperature data for the
(Zr-10Wt%Nb)-H 0.0527 alloy

Temperature °C	Decomposition pressure in mm Hg	Composition at % H	Interpolated decomposition pres- sure for constant composition of the alloy (5.00 at % H)
425.0	8.26×10^{-4}	4.997	8.26×10^{-4}
450.0	2.25×10^{-3}	4.988	2.25×10^{-3}
475.0	5.81×10^{-3}	4.964	5.81×10^{-3}
490.0	9.10×10^{-3}	4.944	9.20×10^{-3}
500.0	1.23×10^{-2}	4.923	1.30×10^{-2}
525.0	2.78×10^{-2}	4.895	2.81×10^{-2}
540.0	3.85×10^{-2}	4.877	4.00×10^{-2}
550.0	4.56×10^{-2}	4.864	4.60×10^{-2}
575.0	5.52×10^{-2}	4.848	6.00×10^{-2}
600.0	6.40×10^{-2}	4.833	7.00×10^{-2}
625.0	7.76×10^{-2}	4.81	8.80×10^{-2}
650.0	1.17×10^{-1}	4.743	1.38×10^{-1}
675.0	1.64×10^{-1}	4.663	2.0×10^{-1}

Table 6

Decomposition Pressure-Composition-Temperature data for the
(Zr-10Wt% Nb) - H 0.0613 alloy

Temperature °C	Decomposition pressure in mm Hg	Composition at % H	Extrapolated decomposition press- ure for constant composition of the alloy (5.78 at % H)
425.0	8.95×10^{-4}	5.771	8.95×10^{-4}
450.0	2.37×10^{-3}	5.762	2.37×10^{-3}
475.0	5.67×10^{-3}	5.742	5.67×10^{-3}
490.0	9.10×10^{-3}	5.721	9.30×10^{-3}
500.0	1.290×10^{-2}	5.698	1.30×10^{-2}
525.0	3.21×10^{-2}	5.582	2.90×10^{-2}
525.0*	2.73×10^{-2}	5.585	
540.0	4.54×10^{-2}	5.556	4.80×10^{-2}
550.0	5.12×10^{-2}	5.547	5.20×10^{-2}
575.0	6.50×10^{-2}	5.524	6.60×10^{-2}
600.0	7.94×10^{-2}	5.500	8.00×10^{-2}
625.0	1.17×10^{-1}	5.439	1.30×10^{-1}
650.0	1.643×10^{-1}	5.363	1.90×10^{-1}
666.0	2.04×10^{-1}	5.298	2.40×10^{-1}

* Data taken during cooling run

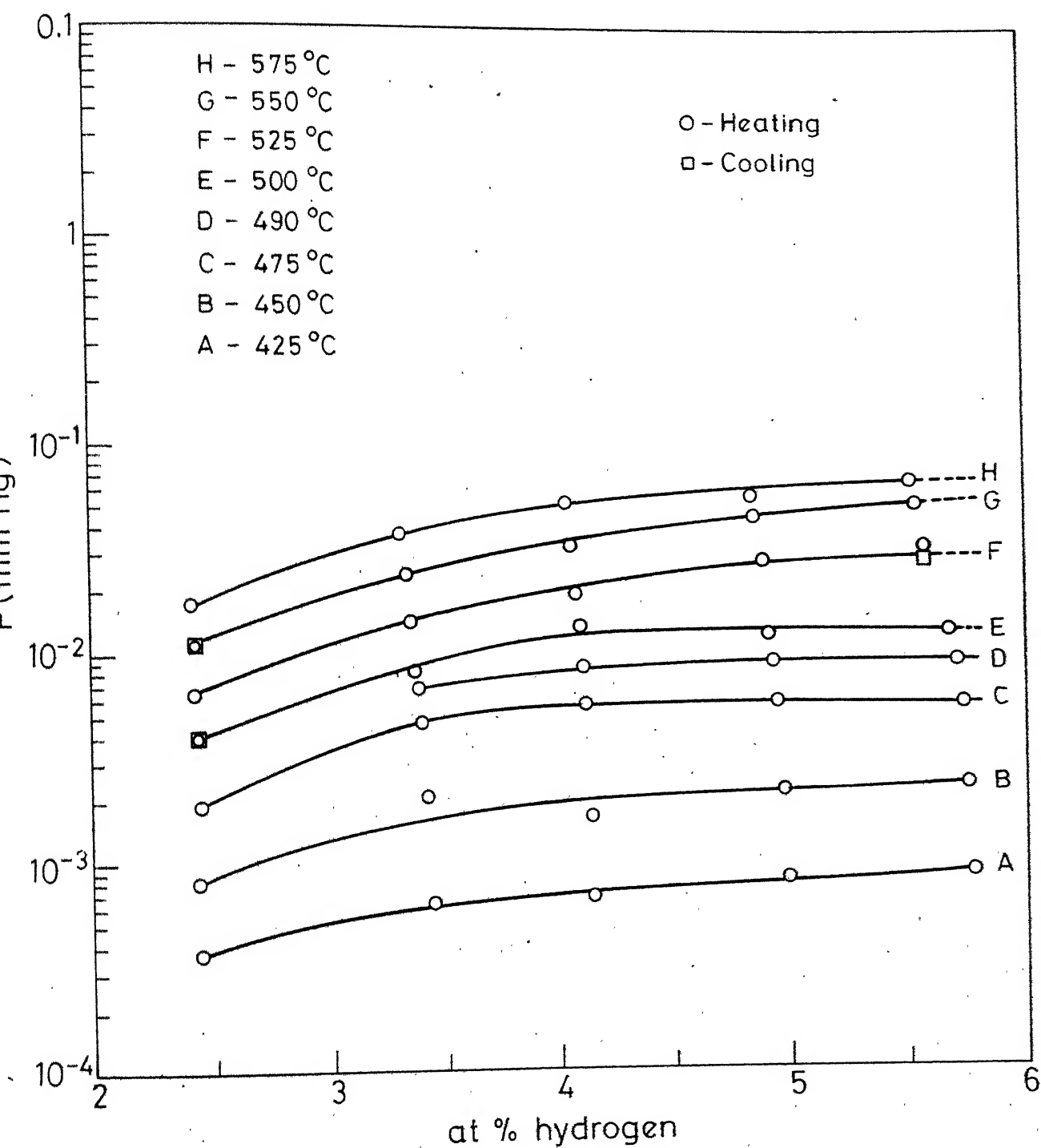


Fig. 2 Isothermal pressure against at% hydrogen for Zr-10wt%Nb alloy in temperature range 425 to 575 °C

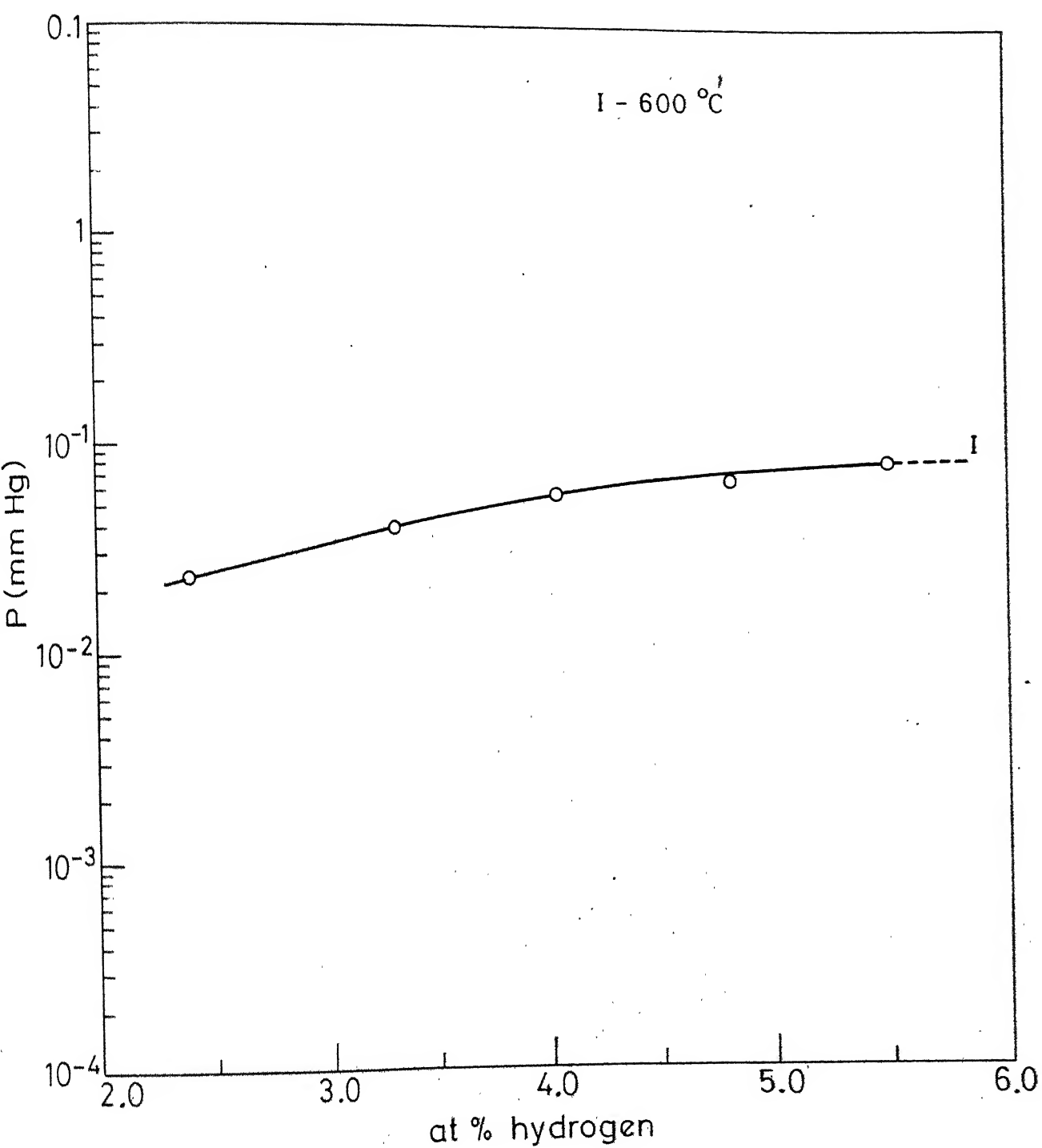


Fig.3 Isothermal pressure against at% hydrogen for Zr-10wt% Nb alloy at 600 °C.

and pressure; the interpolation of the decomposition pressures, in a particular alloy, at constant hydrogen concentration was required. For this purpose, the isothermal values of decomposition pressures, in various alloys are plotted as a function of hydrogen concentration (Fig. 2 and 3). Interpolated values of decomposition pressure (P), at various temperatures were obtained from these plots. Decomposition pressures thus obtained were used for Van't Hoff plots.

4.2 Terminal Solid Solubility of Hydrogen in Zr-10Wt% Nb Alloy:

The plots of $\ln P$ Vs $1/T$ for five, (Zr-10Wt%Nb)-H₂ alloys are shown in Figure 4, 5, 6 and 7. In each plot, the point of inflexion defined a phase transition. For example in Figure 6, the plot for alloy No. 4 depicts that a three* phase region ($\alpha + \beta_{Nb} + \delta$) is stable over the section AB, whereas a two phase region ($\alpha + \beta_{Nb}$) is stable over the section BC. In this alloy and in alloy No. 5, an additional phase transition occurs; which is defined by section CD in Fig. 6. Since the present investigation was aimed, only to determine TSS boundary; no attempts were made to fully determine this phase region in other alloys.

The temperature of TSS boundary in a particular (Zr-10Wt%Nb)-H₂ alloy was determined by intersection of $\ln P$ Vs $1/T$ line in ($\alpha + \beta_{Nb}$) region with a least square line based on average data for ($\alpha + \beta_{Nb} + \delta$) region in all the alloys.

The TSS boundary data obtained on five (Zr-10Wt % Nb)-H₂ alloys are listed in Table 7 and are plotted in Figure 8. For

* The third phase δ_{H_2} comes into picture because of presence of

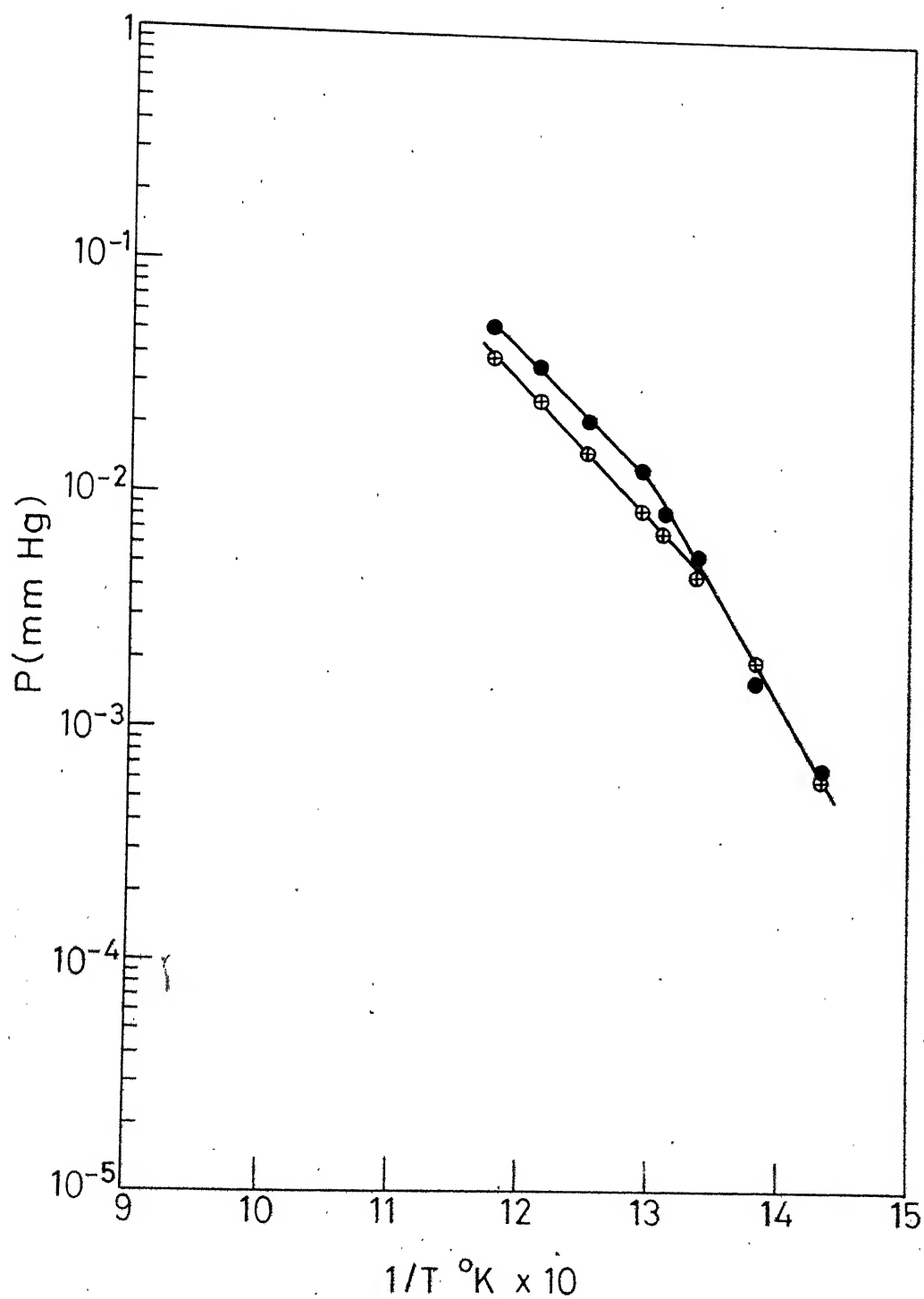


Fig.4 Plot of decomposition pressure Vs. reciprocal of temperature. ● $(\text{Zr-10wt\%Nb})\text{H}_{0.0433}$ alloy, ⊕ $(\text{Zr-10wt\%Nb})\text{H}_{0.0356}$ alloy.

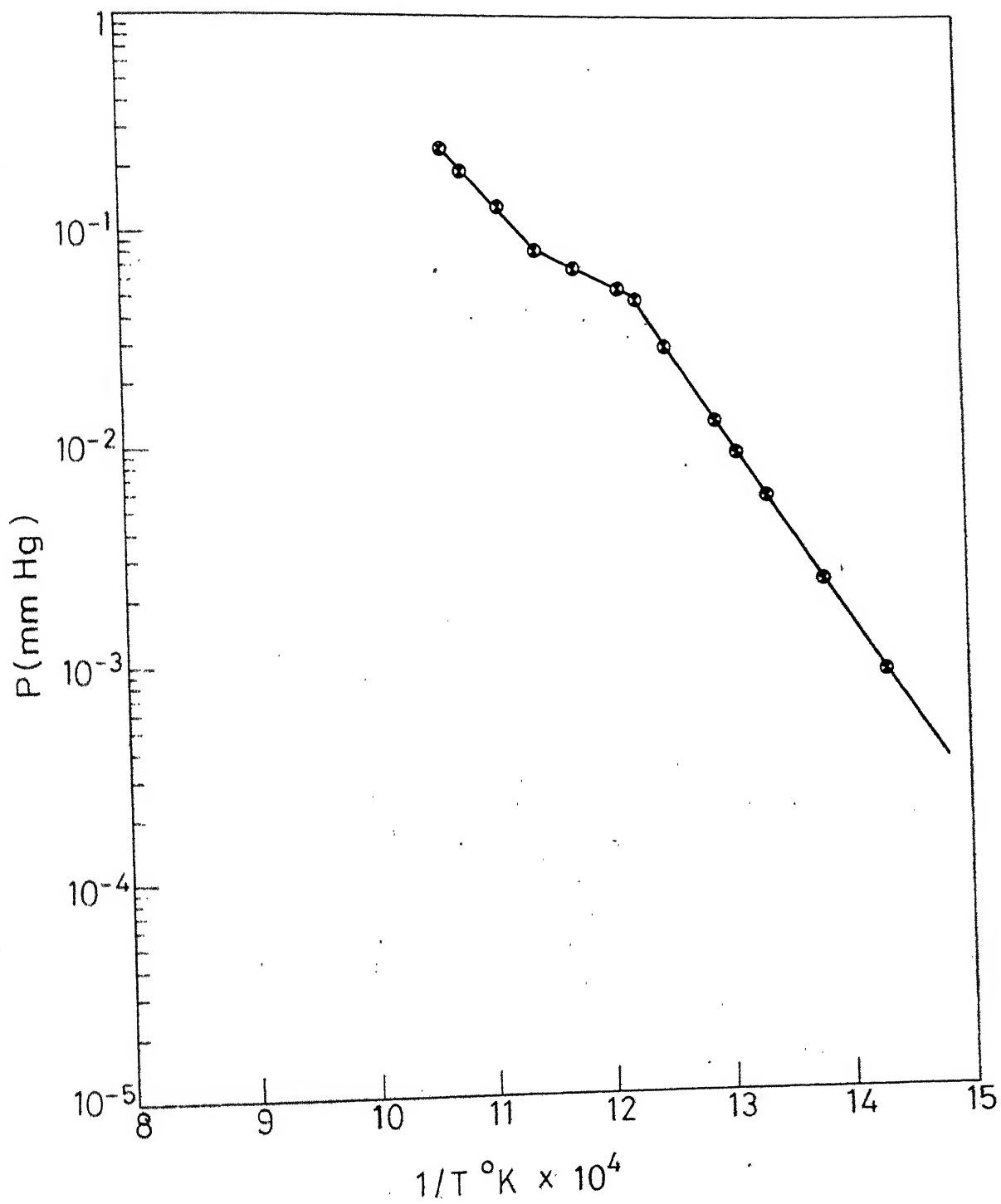


Fig.5 Plot of decomposition pressure Vs. reciprocal of temperature. • (Zr-10 wt%Nb) $\text{H}_{0.0613}$ alloy.

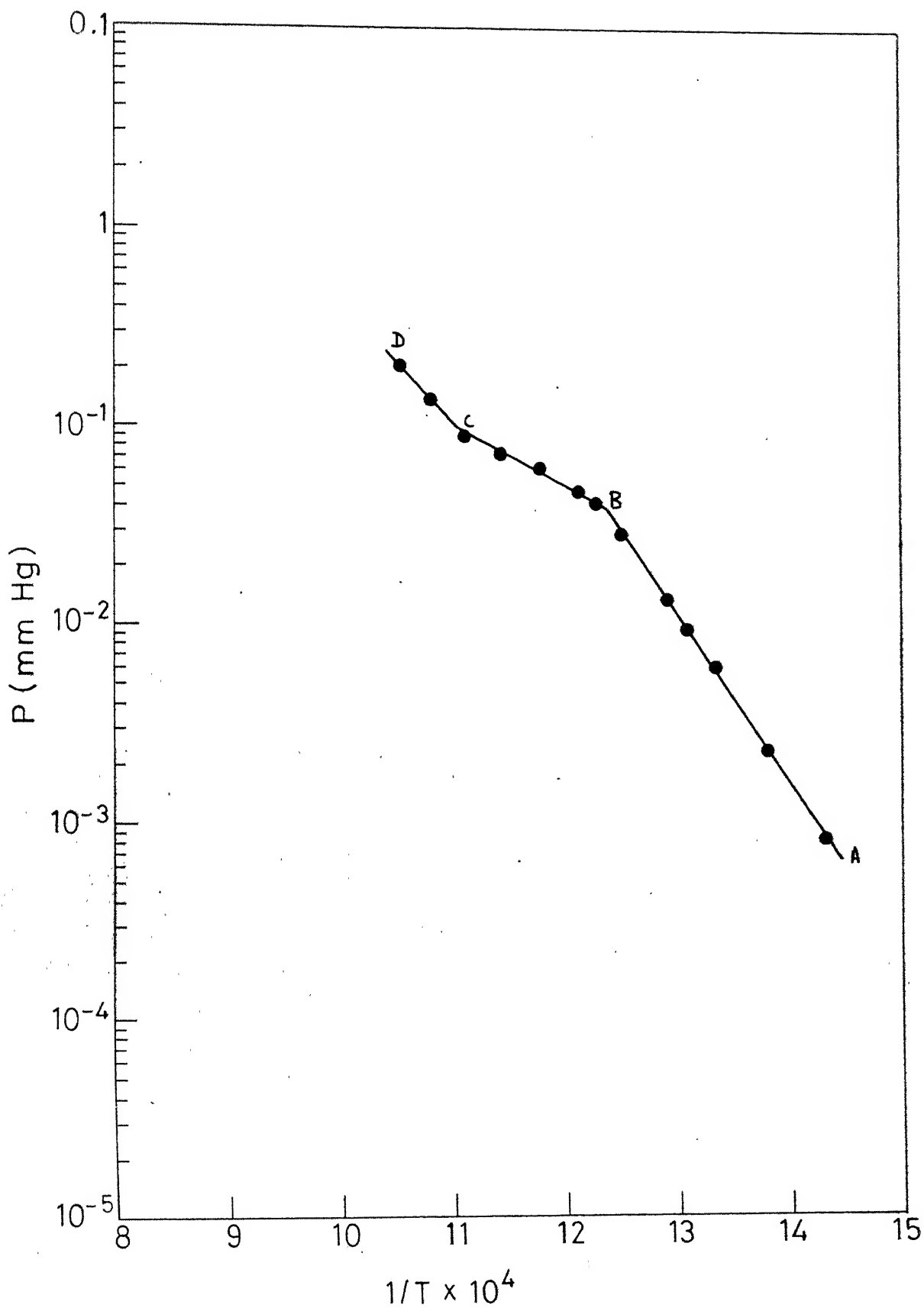


Fig. 6 Plot of decomposition pressure Vs. reciprocal of temperature. • (Zr-10 wt%Nb) $H_{0.0527}$ alloy.

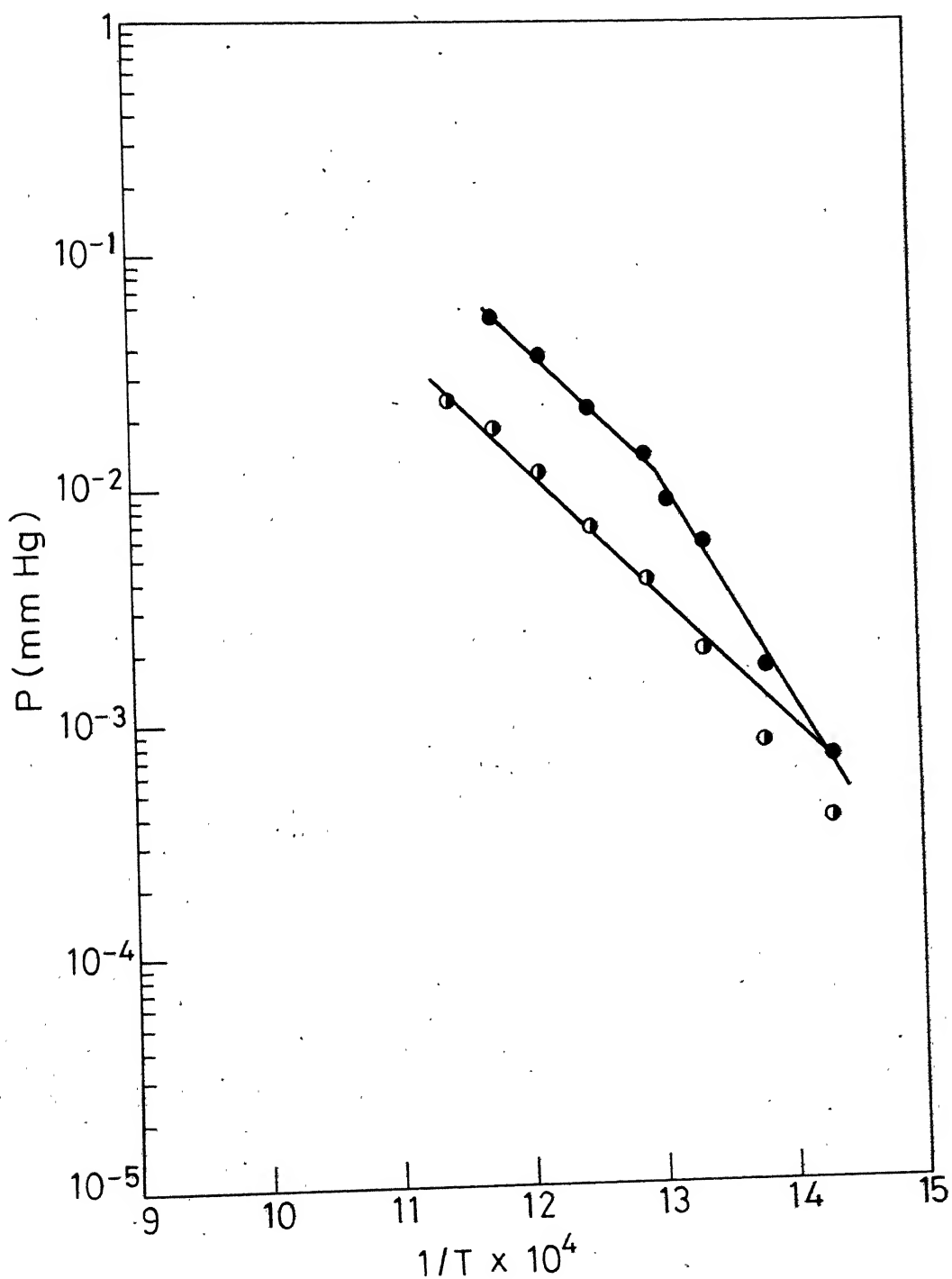


Fig.7 Plot of decomposition pressure Vs.reciprocal of temperature . ● $(Zr-10 \text{ wt\%Nb})H_{0.0433}$ alloy and ○ $(Zr-10 \text{ wt\%Nb})H_{0.0251}$ alloy.

Table 7

Terminal Solid Solubility (TSS) of Hydrogen in the Zr-10Wt% Nb Alloy

Alloy No.	Zirconium-10Wt% niobium)-hydrogen alloy	Composition in at % hydrogen	Temperature in °C for equilibrium TSS ($\alpha + \beta$ Nb + δ) - ($\alpha + \beta$ Nb) boundary.
1	(Zr-10Wt%Nb)-H 0.0251	2.45	413
2	(Zr-10Wt%Nb)-H 0.0356	3.44	469
3	(Zr-10Wt%Nb)-H 0.0433	4.15	502
4	(Zr-10Wt%Nb)-H 0.0527	5.00	534
5	(Zr-10Wt%Nb)-H 0.0613	5.78	541

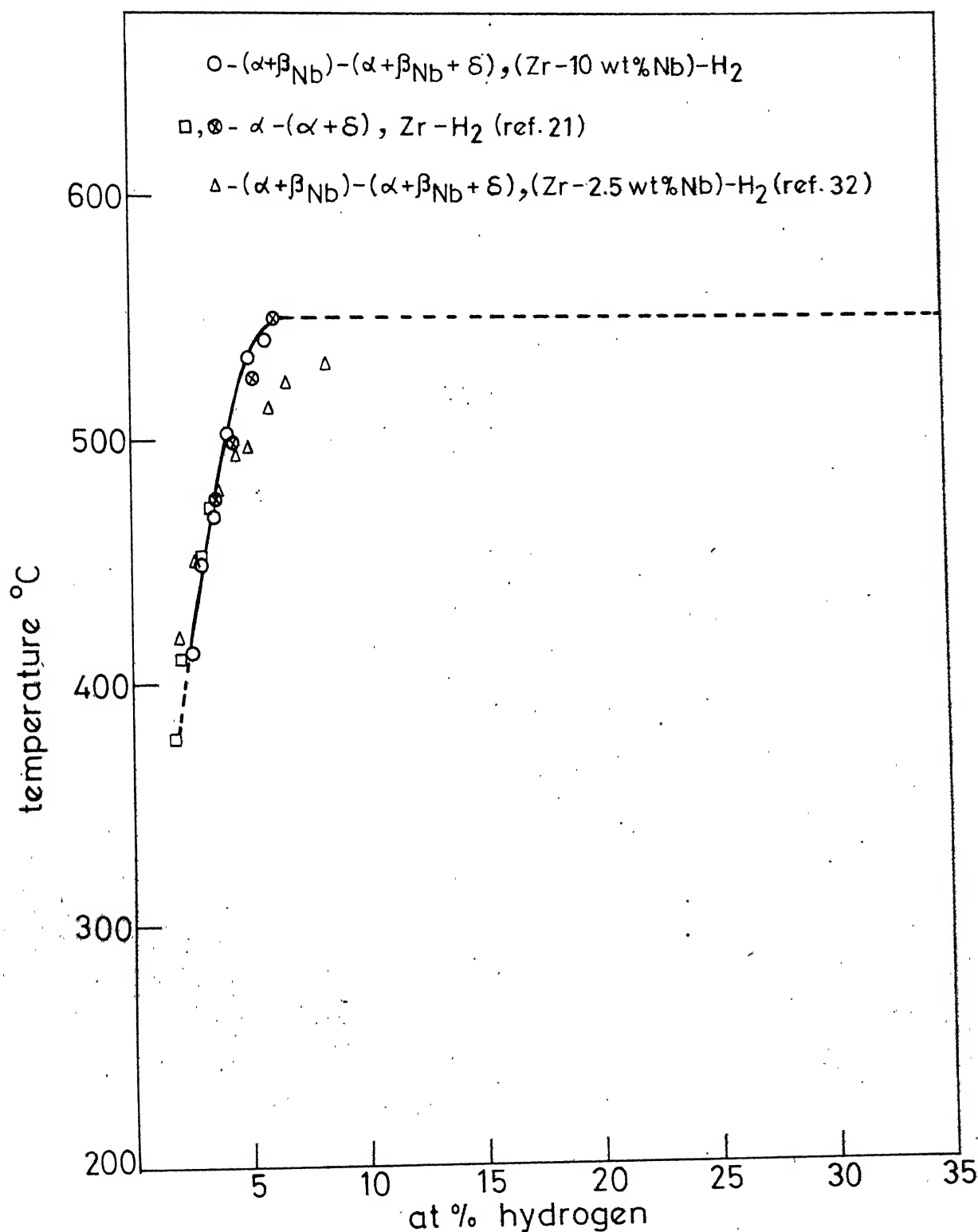


Fig. 8 TSS boundaries $(\alpha + \beta_{\text{Nb}}) - (\alpha + \beta_{\text{Nb}} + \delta)$ for the $(\text{Zr-2.5 wt\% Nb})-\text{H}_2$, $(\text{Zr-10 wt\%Nb})-\text{H}_2$ systems; and $\alpha - (\alpha + \delta)$ for $\text{Zr}-\text{H}_2$ system. \circ -present work on $(\text{Zr-10 wt\%Nb})-\text{H}_2$ system, \triangle Sinha (32), \square Gulbransen et al van't Hoff plot (ref. 21) \otimes Gulbransen et al Sieverts law plot (ref. 21).

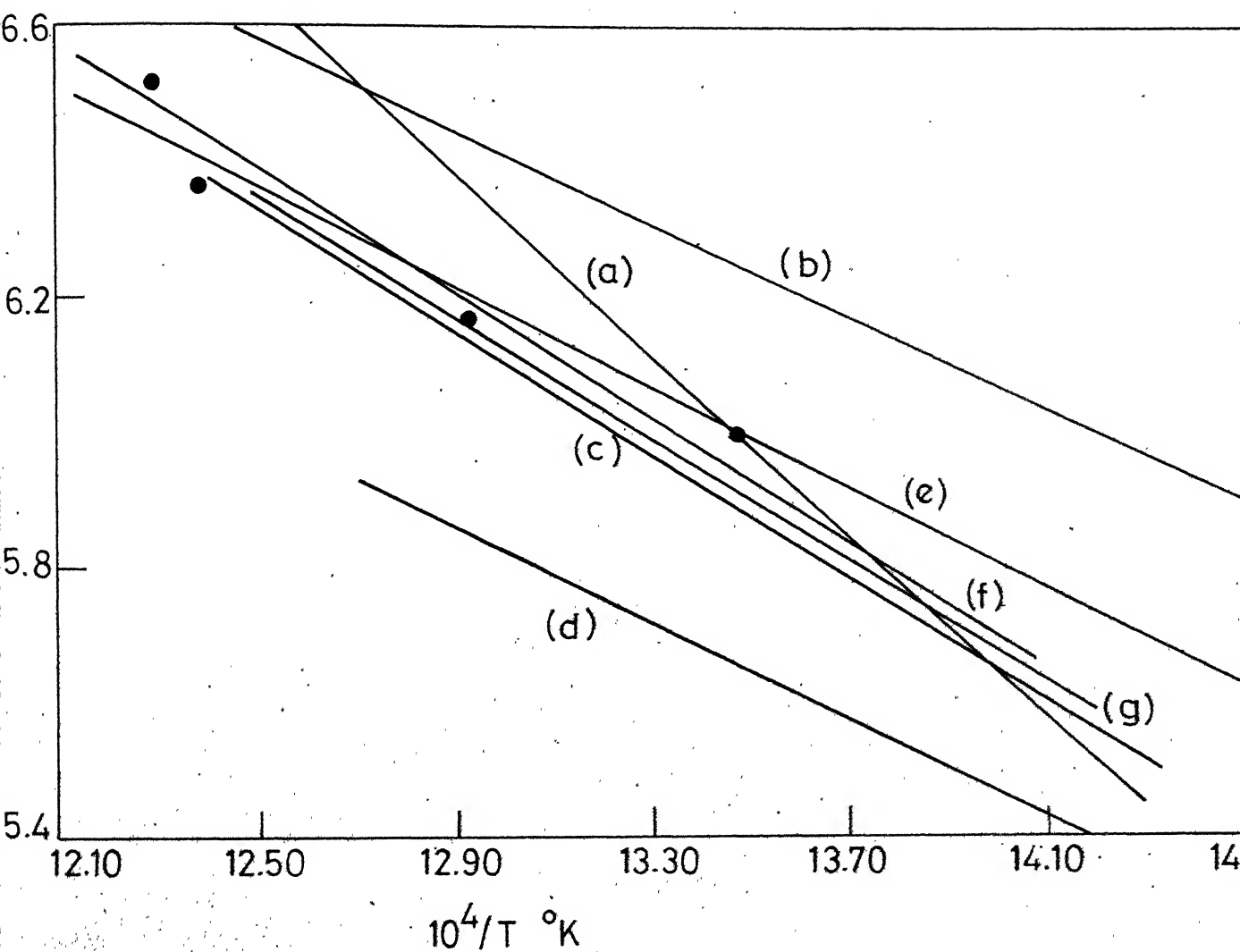


Fig. 9 Plot of $\ln C_T$ against $1/T$ °K for $(\alpha+\beta_{Nb})-(\alpha+\beta_{Nb}+\delta)$ TSS boundary in the $(Zr-2.5\text{wt}\%Nb)-H_2$ and $(Zr-10\text{wt}\%Nb)-H_2$ systems; and $\alpha-(\alpha+\delta)$ TSS boundary in $Zr-H_2$ system.

$(Zr-2.5\text{ wt } \%Nb)-H_2$ system :-

(a) Sinha (ref 32), (b) Erickson (ref.18), (c) Sawatzky et al (ref. 19),
(d) Slattery (ref. 20).

$(Zr-10\text{ wt } \%Nb)-H_2$ system :- (e) • present work.

$Zr-H_2$ system :-

(f) Gulbransen et al (ref.21) (g) Kearns (ref.28)

comparison the TSS data of hydrogen in unalloyed zirconium⁽²¹⁾ and in Zr-2.5Wt% Nb⁽³²⁾ are also plotted. The addition of 10Wt% Nb to Zr, does not seem to affect the TSS of hydrogen in the alloy as compared to unalloyed zirconium. This observation as to the effect of niobium on TSS of hydrogen in zirconium, is in agreement with earlier results^(19,48) on (Zr-2.5Wt%Nb)-H₂ system. Thus the present investigation supports the view^(17,18) that probably presence of niobium does not affect the TSS of hydrogen in zirconium significantly.

Using a least square method the equation to represent the TSS data for hydrogen in Zr-10Wt% Nb alloy, in temperature range 400 to 550°C has been derived to be

$$\ln C_T(\text{ppm}) = 10.94 - 7275/RT \quad \dots \quad 4.2$$

with a standard error of 1 ppm H₂ by weight in C_T. The mean value of enthalpy of solution of δ hydride in saturated ($\alpha + \beta_{\text{Nb}}$) was computed⁽³⁴⁾ to be - 7.3 K.Cal/mole H₂. Gulbransen and Andrew⁽²¹⁾ reported the mean enthalpy of solution of δ hydride in unalloyed α Zr to be equal to - 8.6 K.Cal/gm-mole H₂, which is close to the value obtained in present investigation. This also suggests that TSS of hydrogen in zirconium is not affected appreciably by the presence of 10Wt% niobium. The equation (4.2) is plotted in Figure 9, along with the least square plots of other investigators for the TSS of hydrogen in Zr-2.5Wt% Nb alloy^(18,19,20,32) and unalloyed zirconium^(21,28) for comparison. It can be seen that within experimental errors the TSS of hydrogen in Zr-10Wt% Nb alloy is nearly same as that in unalloyed zirconium.

From the data of Tables 2 to 6; the decomposition pressure and temperature relationship in the $(\alpha + \beta_{\text{Nb}} + \delta)$ region, using a least square method was determined to be

$$\ln P(\text{atm}) = 15.3020 - \frac{40.384 \times 10^3}{RT} \quad \dots \quad 4.3$$

The mean enthalpy of formation of δ hydride from saturated $\alpha + \beta_{\text{Nb}}$, $\Delta \bar{H}_{\alpha \rightarrow \delta}$, was computed to be, -40.4 K.Cal/mole H_2 . The reported values of $\Delta \bar{H}_{\alpha \rightarrow \delta}$, in unalloyed⁽²¹⁾ Zr- H_2 system is, -45.8 K.Cal/mole H_2 and in (Zr-10Wt% Nb)- H_2 system⁽³²⁾ is, -40.9 K.Cal/mole H_2 . The value of $\Delta \bar{H}_{\alpha \rightarrow \delta}$ obtained in present investigation is very close to the value obtained for (Zr-2.5Wt% Nb)- H_2 system⁽³²⁾ and this indicates that probably addition of niobium above 2.5 Wt% does not affect the enthalpy of formation of δ hydride from saturated α zirconium. As per earlier observations⁽⁴⁷⁾ niobium bears a similar affect an enthalpy of formation of ϵ hydride ($\Delta \bar{H}_{\beta \rightarrow \epsilon}$) from saturated β -zirconium.

Several investigators^(16,17,18,19,20,30,32,48) have attempted to establish TSS of hydrogen in Zr-2.5Wt% Nb alloy in order to study the affect of niobium on TSS of hydrogen in zirconium. The results of present investigation on (Zr-10Wt% Nb)- H_2 system confirm the observations made by Sawatzky and Wilkins⁽¹⁹⁾ and Coates & Erickson⁽⁴⁸⁾. Thus it appears that TSS of hydrogen in zirconium is not affected appreciably by the presence of 10Wt% niobium. However other investigators^(16,17,18,30,32) found that TSS of hydrogen in Zr-2.5Wt% Nb alloy is somewhat higher than unalloyed zirconium. Sinha⁽³²⁾ indicated that the higher TSS of hydrogen in Zr-2.5Wt% Nb

alloy may be attributed to the formation of some Zr-Nb-H_2 complex analogous to the Zr-Ni-H_2 system⁽⁵⁰⁾; but so far there are no experimental or theoretical evidences as to prove the presence of such complex. On the other hand it seems more probable that because of higher decomposition pressures of hydrogen in niobium⁽⁵¹⁾ the TSS equilibria in a $(\text{Zr-10Wt\% Nb})\text{-H}_2$ system is predominantly governed by zirconium only. Therefore addition of 10Wt% niobium does not appreciably affect the TSS of hydrogen in zirconium.

CHAPTER V

CONCLUSIONS

Following conclusions can be made on the basis of present investigation:

1. The addition of 10Wt%Nb does not seem to affect the terminal solid solubility of hydrogen in Zr significantly, and within experimental errors the TSS of hydrogen in Zr-10Wt% Nb and in unalloyed Zr is same.
2. The enthalpy of solution of δ hydride in saturated α Zr in the Zr-10Wt% Nb alloy is close to that in unalloyed zirconium. Therefore the enthalpy of solution of δ hydride in saturated α zirconium is not very sensitive to the presence of 10Wt% Nb in the alloy.
3. The enthalpy of formation of δ hydride from saturated α Zr, $\Delta \bar{H}_{\alpha \rightarrow \delta}$, is insensitive to the increase of niobium content of the alloy above 2.5 Wt% Nb.

REFERENCES

1. Etherington et. al, in "The Metallurgy of Zirconium" ed. B.Lustman and F. Kerze, Jr. McGraw-Hill, New York, 1955, Chap. 1. P.5.
2. R.L. Beck & W.M. Mueller, "Metal Hydrides", eds. W.M. Mueller, J.P. Bleckledge & G.G. Libowitz, Academic Press, 1968, Chap. 7.
3. K. Balaramamurthy, "Symposium on Non-Ferrous Metallurgy", Vol.III, eds. J.E. Manner and P.K. Gupta, N.M.L. Jamshedpur, India, 1968, p. 181.
4. B.G. Parfenov, V.V. Gerasimov, and G.I. Venediktova, "Corrosion of Zirconium and Zirconium Alloys", Israel Programme for Scientific Translations, Jerusalem, 1969, P.5.
5. R.S. Ambartsumyan et. al, "Proceedings of 2nd ICPUAE", Geneva, Vol. 5 (United Nations, 1958), P. 12.
6. O.S. Ivanov and V.K. Grigorovich, *ibid*, Vol. 5, p. 34.
7. C.R. Cupp, "J. Nucl. Materials", 6 (1962), 241.
8. W.Evans, L.G. Bell, Report No. AECL 1395, 1961.
9. J.H. Foley, "Heavy Water Reactor International News Letter", Chalk River Ontario, No. 6, 1963.
10. G.F. Slattery, "J. Less Comm. Metals", 8 (1965), 195.
11. P.Cotterill, "Progress in Materials Science", 2 (1961), 286.
12. C.E. Ells "J. Nucl. Materials", 28 (1968), 129.

14. C.Roy and J.G. Jacques, "J. Nucl. Materials", 31(1969), 233.
15. G.G. Libowitz "Solid State Chemistry of Binary Metal Hydrides",
W.A. Benjamin, Inc., New York.
16. A. Brown, Ph.D. thesis (University of Durham, U.K.), 1961.
17. W.H. Erickson & D. Hardie "J. Nucl. Materials", 13 (1964), 254.
18. W.H. Erickson, "J. Electrochem. Tech.", 4 (1966), 205.
19. A. Sawatzky & B.J.S. Wilkins, "J. Nucl. Materials", 22 (1967), 304.
20. G.F. Slattery, "J. Inst. Metals", 95 (1967), 43.
21. E.A. Gulbransen & K.F. Andrew, "J. Metals", 7 (1955), 136.
22. C.E. Ells & A.D. McQuillan, "J. Inst. Metals", 85 (1956), 89.
23. L. Espagno, P. Azou and P. Bastein, "Compt. Rend.", 249 (1959), 20003
24. T.B. Douglas, "J. Amer. Chem. Soc.", 80 (1958), 5040.
25. R.L. Beck & W.M. Mueller, "Metal Hydrides", eds. W.M. Mueller, J.P.
Blackledge and G.G. Libowitz, Academic Press, 1968, Chap. 7, p. 255.
26. M.W. Mallet and W.M. Albrecht, "J. Electro Chem. Soc.", 104(1957), 142
27. C.M. Schwartz and M.W. Mallet, "Amer. Soc. Metals", Trans. Quart.,
46 (1954), 640.
28. J.J. Kearns, "J. Nucl. Materials", 22 (1967), 292.
29. L.D. La Grange, L.J. Dykstra, J.M. Dixon and U. Merteen, "J. Phys.
Chem.", 63 (1959), 2035.
30. A. Sawatzky "Quotes as Private Communication in Ref. 18".
31. H.H. Klepfer, "J. Nucl. Materials", 2 (1963), 77.

32. V.K. Sinha, (Ph.D. thesis, I.I.T, Kanpur), 1973.
33. A.D. McQuillan "J. Inst. Metals", 79 (1951), 371.
34. D.G. Westlake, "J. Nucl. Materials", 1 (1962), 346.
35. G. Hagg, "Rontgenuntersuchungen über die Hydride Von Titan ,
Zirkonium, Vanadin and Tantal, "Z. Phys. Chem.", B, 11(1930), 433.
36. Hall et al., "Trans. Faraday. Soc. ", 41 (1945), 306.
37. Edwards et. al, "J. Amer. Chem. Soc.", 77 (1955), 1307.
38. Edwards & Levesque, "J. Amer. Chem. Soc.", 77 (1955), 1312.
39. E.A. Gulbransen & K.F. Andrew, "J. Electrochem. Soc.", 101(9)
(1954), 474.
40. Vaughan and Bridge, "J. Metals", 8(5) (1956), 528.
41. G.G. Libowitz, "J. Nucl. Materials", 5 (1962), 228.
- 42(a) R.L. Beck, "Amer.Soc. Metals", Trans Quart., 55 (1962), 542,
(b) R.L. Beck, ibid, 55 (1962), 556.
43. S. Mishra, K.S. Sivaramakrishnan & M.K. Ausundi, "J. Nucl.Materials"
45 (1972/73), 235.
44. Brown & Hardie, "J. Nucl. Materials", 4 (1961), 110.
45. K.P. Singh, J.G. Parr, "Trans. Faraday Soc.", 59(1963), 2248.
46. V.K. Sinha & K.P. Singh, "J. Nucl. Materials", 36 (1970), 211.
47. V.K. Sinha & K.P. Singh, "Met. Trans.", 3 (1972), 1581.
48. D.E. Coates & W.H. Erickson- "Quoted as Unpublished work in Ref.18".
49. Moore & Young", J. Nucl. Materials", 27 (1968), 316.
50. G.G. Libowitz, H.F. Hayes & T.R.P. Gibb, Jr."J. Phys. Chem.",
62 (1958), 76.

51. W.M. Albrecht, W.D. Goode & M.W. Mallet, "J. Electrochem. Soc.",
106 (1959), 981.
52. R.P. Elliot, "Constitution of Binary Alloys", McGraw Hill, 1965,
p. 279.
53. F.A. Shunk "Constitution of Binary Alloys", Mc Graw Hill, 1969,
p. 184.

A P P E N D I X

Appendix

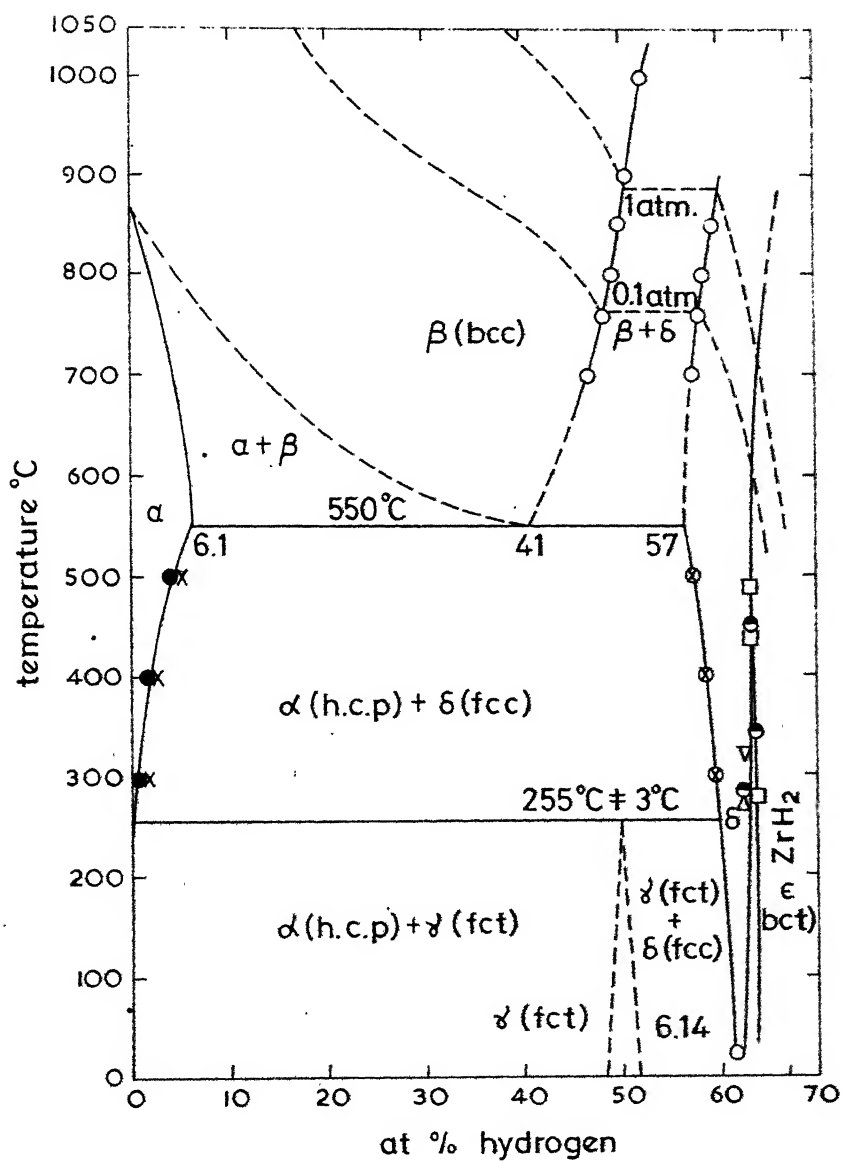


Fig. 10. The equilibrium phase relations in zirconium-hydrogen system.

x, Schwartz et al (ref 27); o, Beck (ref 42);
 ●, Gulbransen et al (ref 21); ⊙, Espagno et al
 (ref 23); □ Δ ▽, Moore et al (ref 49)

Appendix

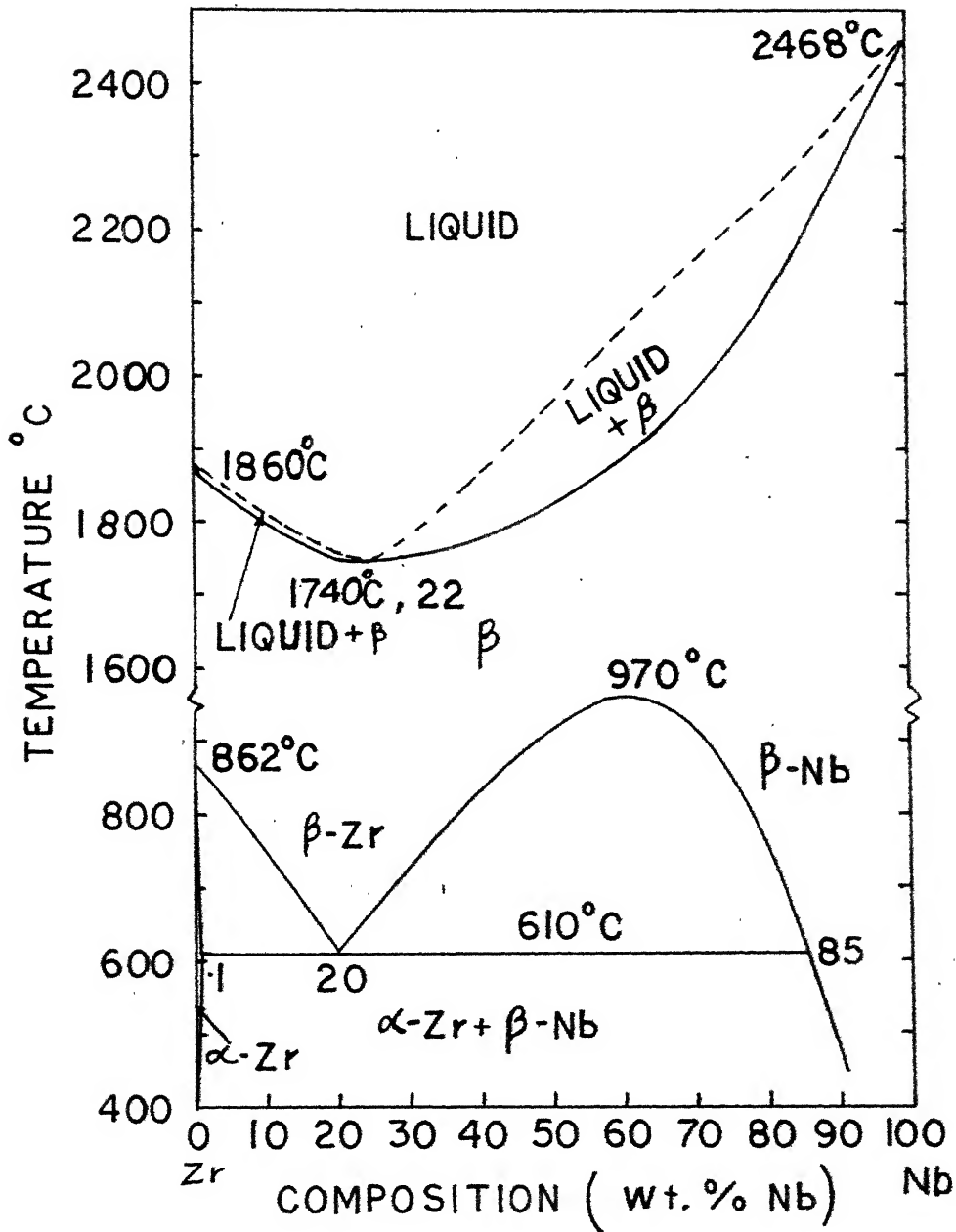


FIG. 11 . THE EQUILIBRIUM PHASE DIAGRAM OF Zr-Nb SYSTEM.

Appendix

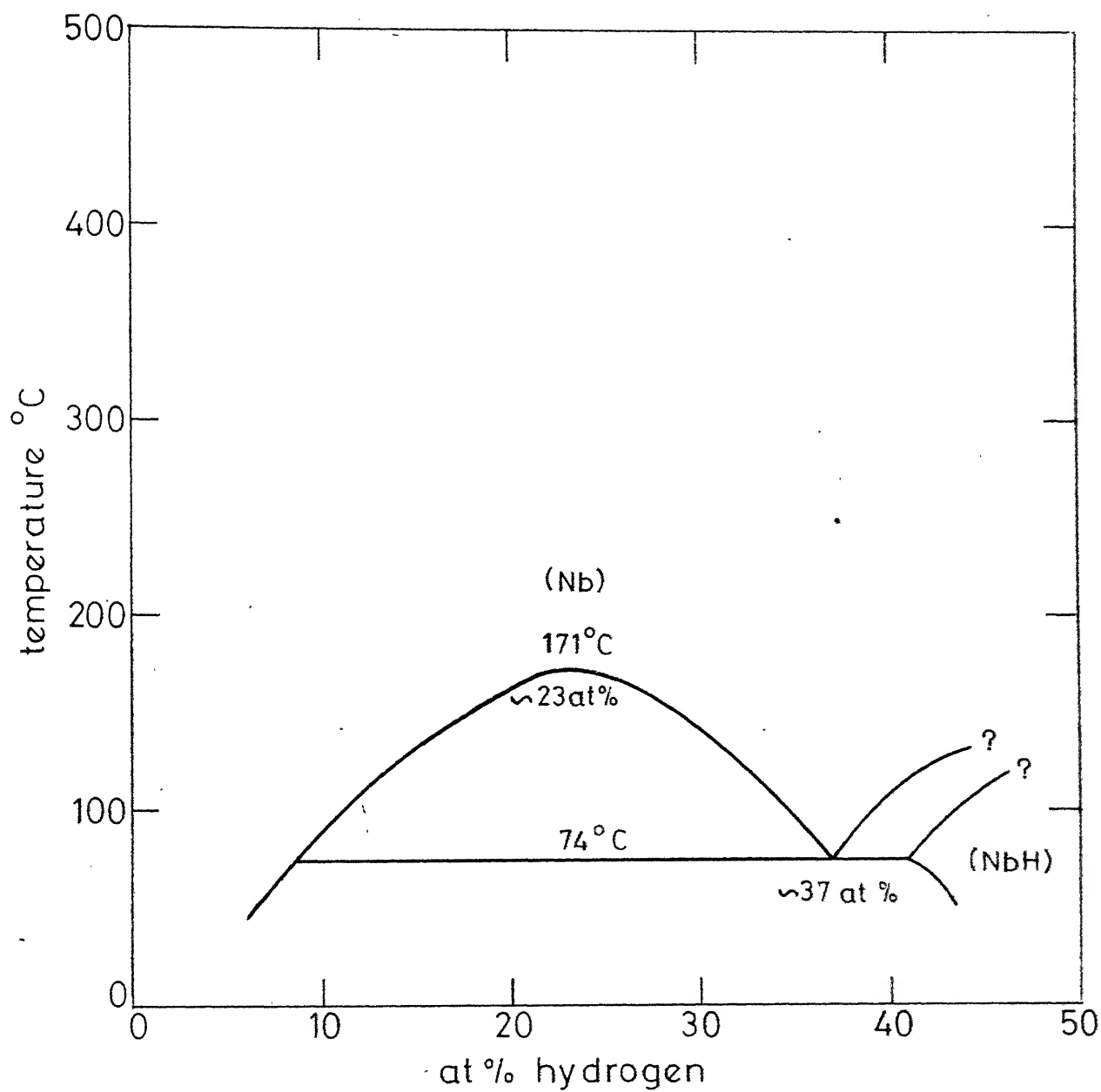


Fig.12 The equilibrium phase relations in niobium-hydrogen system.